Searching for Super Hard Cubic Phases of Cubic Transition Metal Nitrides from *Ab Initio* Computations

Sanjay V. Khare

Department of Physics and Astronomy
University of Toledo
Ohio 43606
http://www.physics.utoledo.edu/~khare/

General theme of our research

Static

- Energetic, thermodynamic, electronic, and structural properties related to materials phenomena.

Dynamic

- Near equilibrium and non-equilibrium mass transport mechanisms at surfaces.

Techniques

- Use of appropriate theoretical and computational techniques.

Touch with reality

- Direct contact with experiments through explanations, predictions, and direction for future experimental work.

Our other research (not presented today)

- Diffusion in Semiconductors
- Diffusion on GaAs(001) surfaces – work with Prof. Ray Phaneuf
- Diffusion in bulk CdTe

Photovoltaic Materials

- β-In_2X_3 (X = O, S, Se, Te), β-X_2S_3 (X = In, B, Al, Ga)
- CuZnSnSSe (CZTS, CZTSe), Zn_3N_2

Structural, energetic and electronic properties of Nanowires

- Ge and Si

Global Energy Sources and Consumption for Humans

- US Coal and World Uranium, EROEI

Funding: U of Toledo, Air Force, NSF, DoE

Diffusion of a Ga adatom on the GaAs(001)–c(4×4)–heterodimer surface: A first-principles study

J.L. Roehl[1], S. Aravelli[2], S.V. Khare[1], R.J. Phaneuf[3]

1. **Department of Physics and Astronomy**
University of Toledo, Ohio

2. Department of Electrical Engineering and Computer Science
University of Toledo, Ohio

3. Department of Materials and Nuclear Engineering, University of Maryland, College Park, MD

This work supported by NSF (DMR-0705464, CNS 0855134), Wright Center for PVIC and Ohio Supercomputer Center

Diffusion Path #1

- Along [0 -1 0]
- Crosses 6 Barriers
- Largest Barrier 0.42 eV

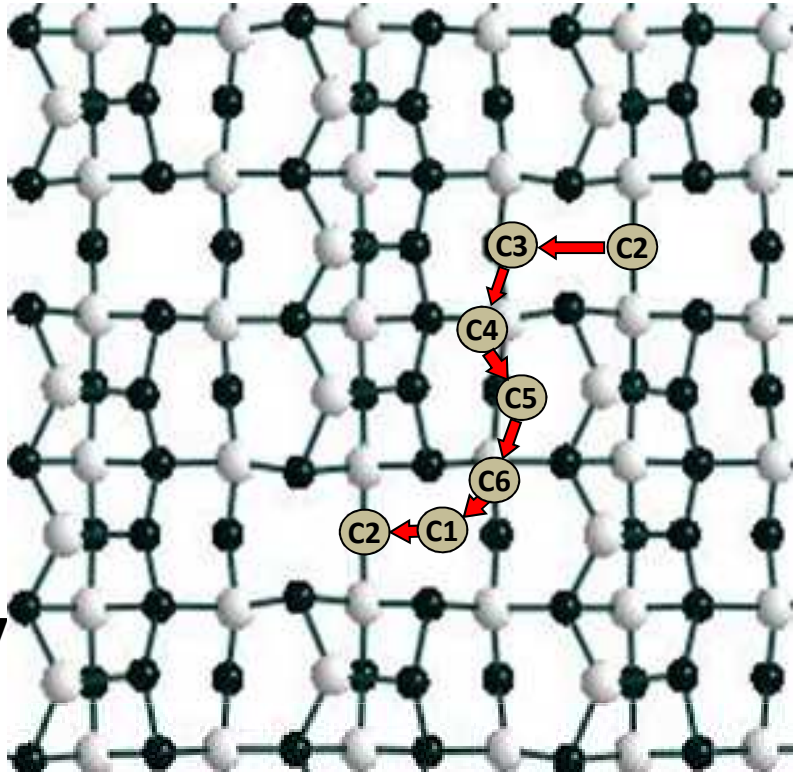

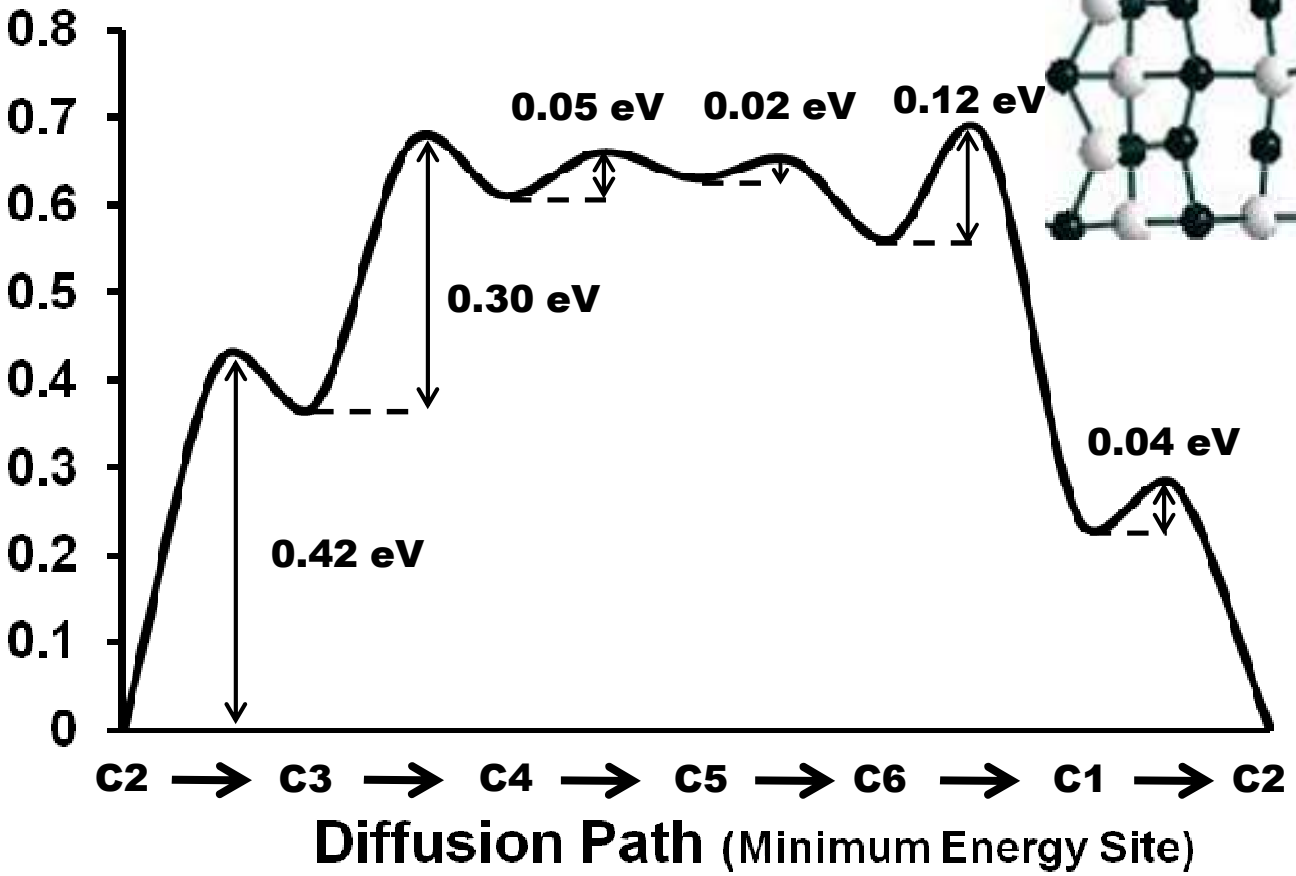

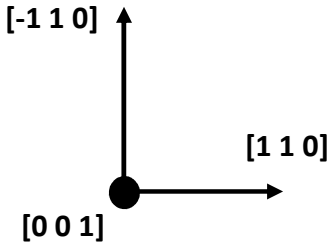

Diffusion Path #2

- Along [-1 -1 0]
- Crosses 5 Barriers
- Largest Barrier 0.42 eV

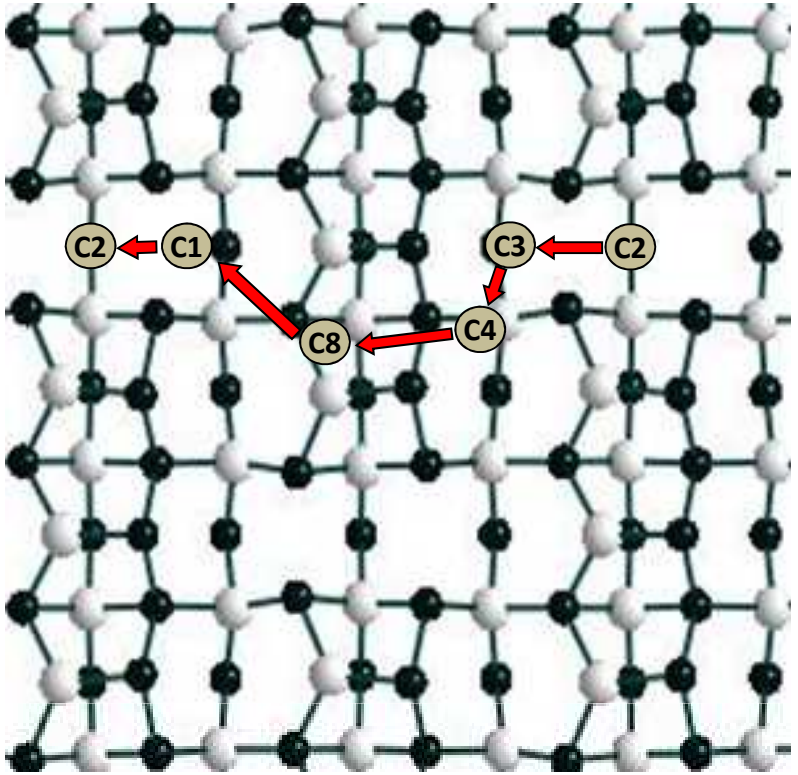

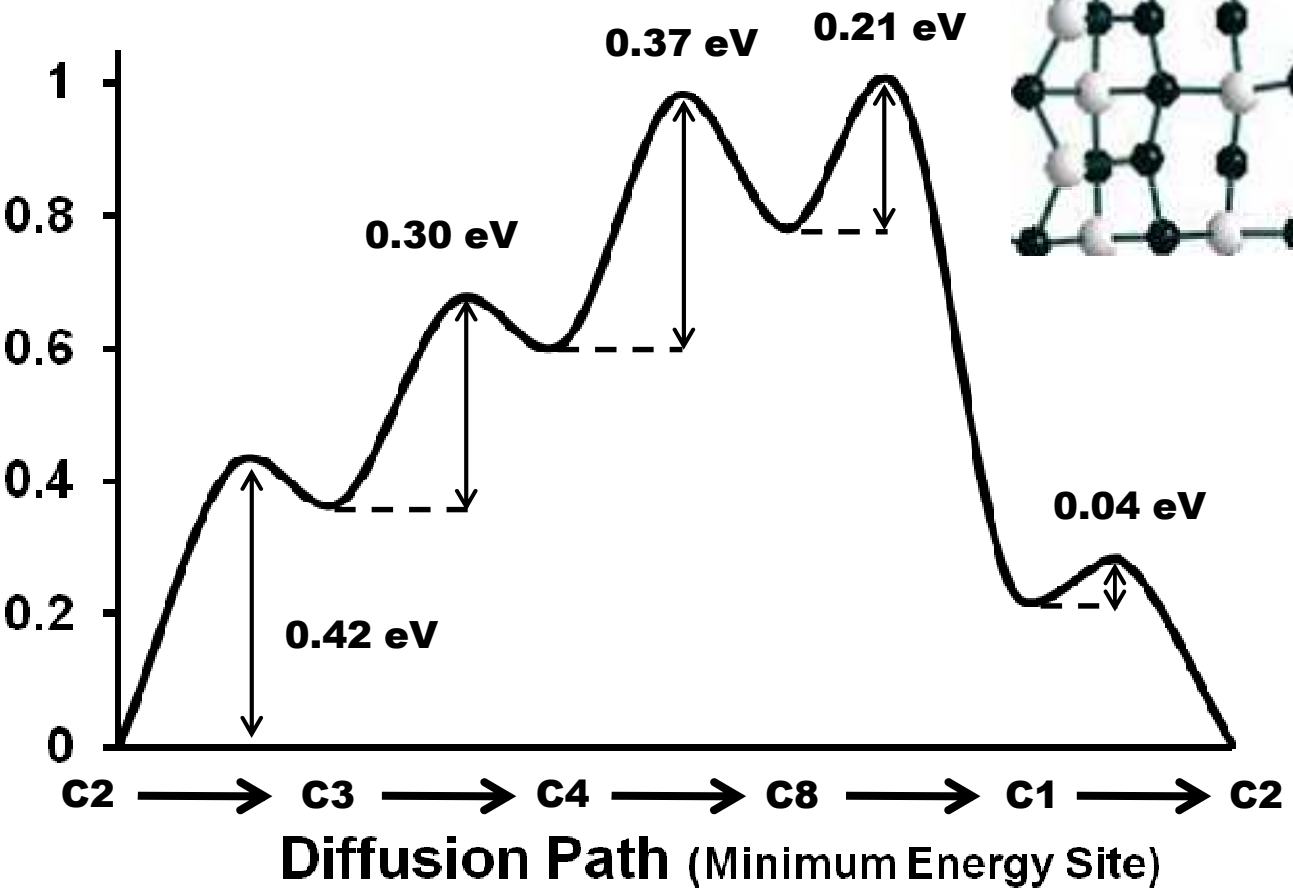

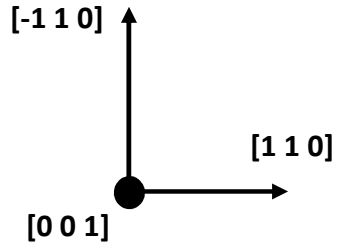

Binding sites and diffusion barriers of a Ga adatom on the GaAs(001)-*c*(4×4) surface from first-principles computations

J.L. Roehl[1], A. Kolagatla[2], V.K.K. Ganguri[2], S.V. Khare[1], R.J. Phaneuf[3]

1. **Department of Physics and Astronomy**
University of Toledo, Ohio

2. Department of Electrical Engineering and Computer Science
University of Toledo, Ohio

3. Department of Materials and Nuclear Engineering, University of Maryland, College Park, MD

This work supported by NSF (DMR-0705464), Wright Center for PVIC and Ohio Supercomputer Center

Diffusion Path #1

- Crosses 4 Barriers
- Largest Barrier 0.46 eV

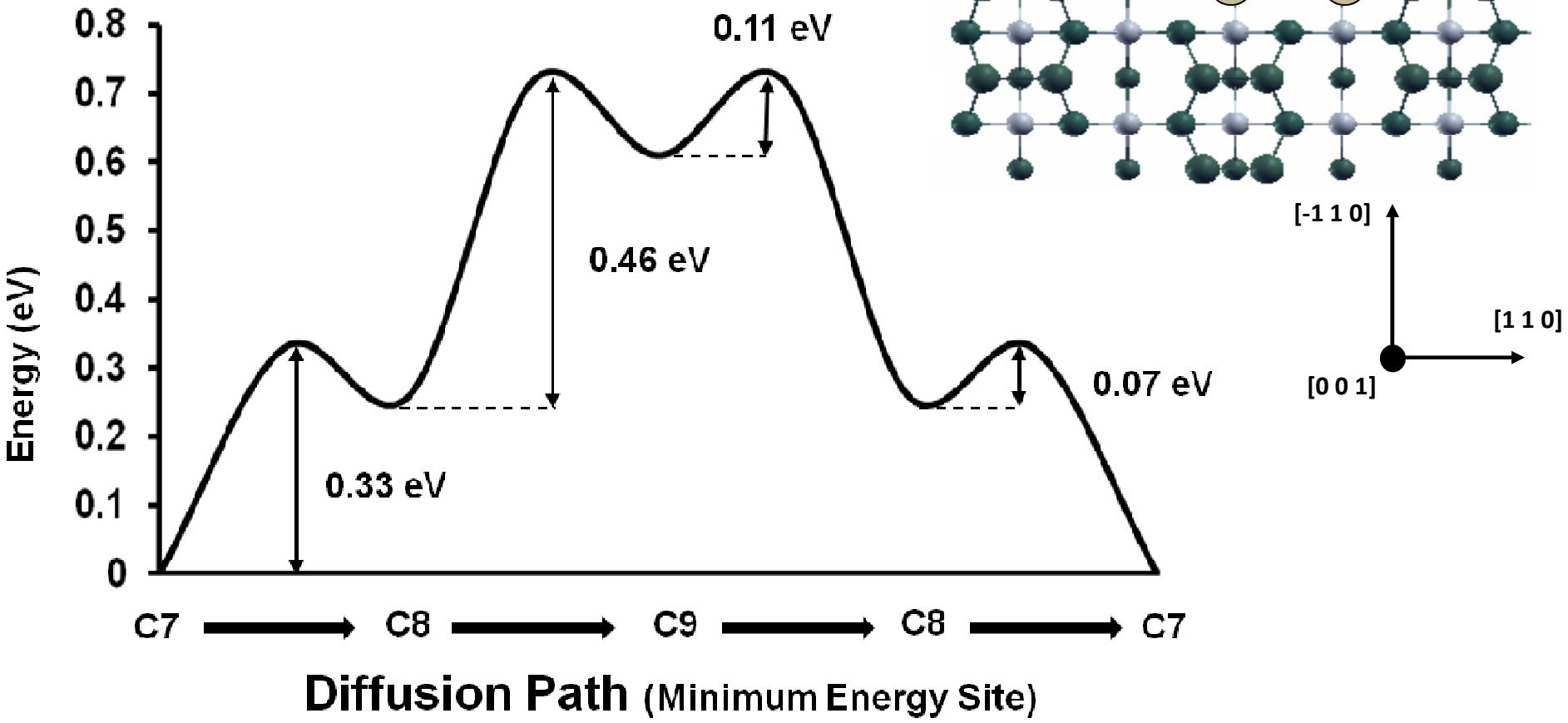

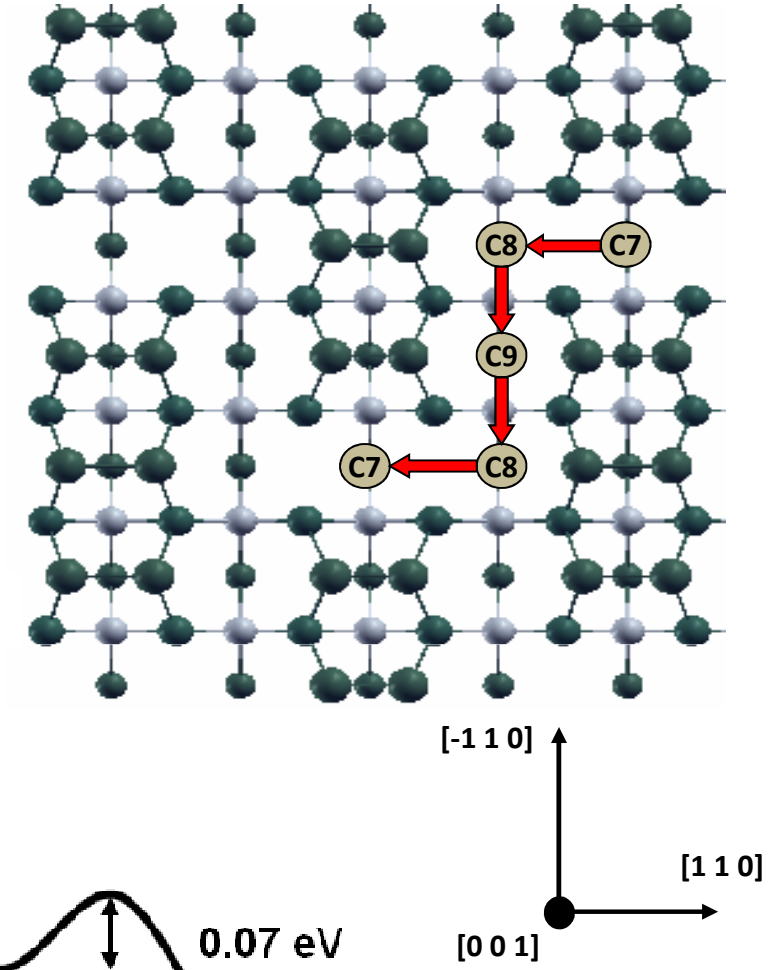

Diffusion Path #2

- Crosses 5 Barriers
- Largest Barrier 0.46 eV

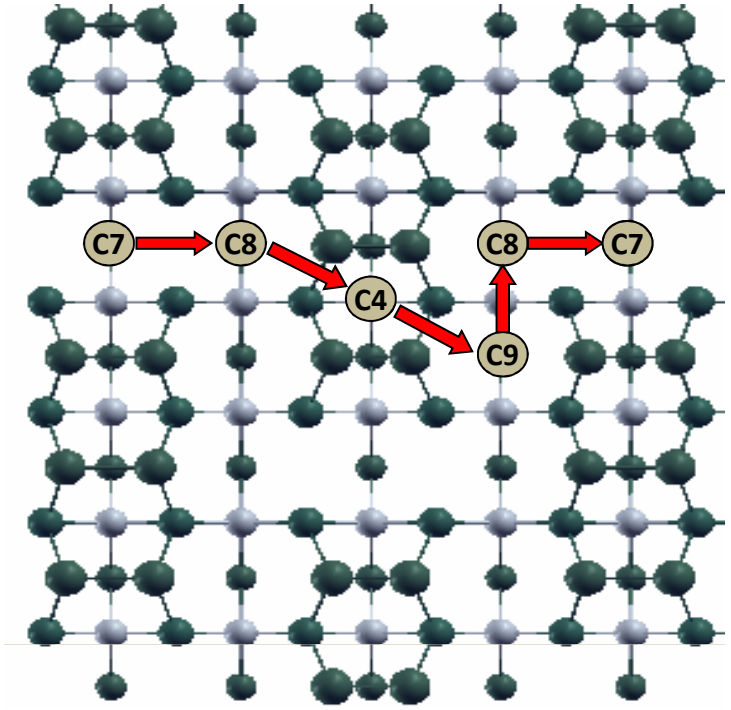

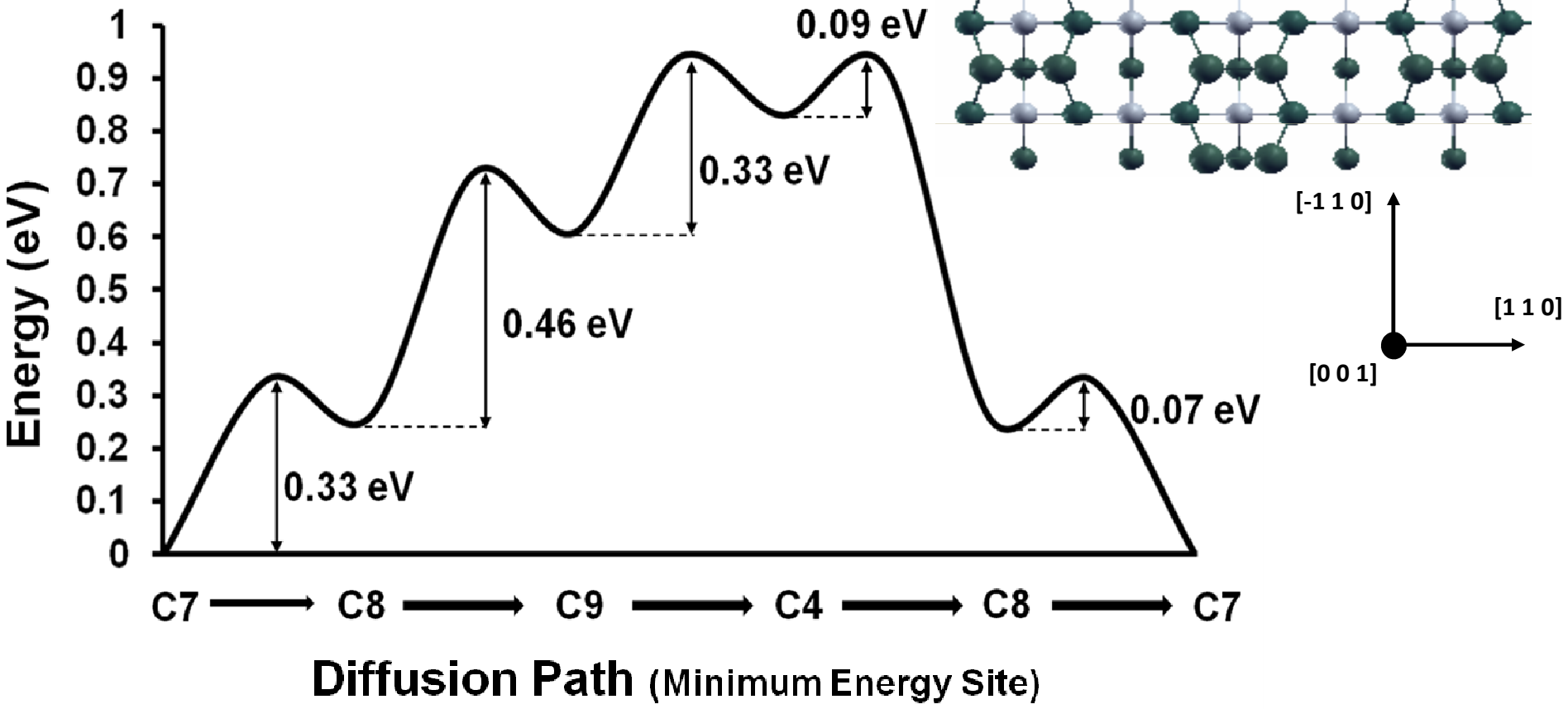

TMN hard coatings, collaborators:

S. K. R. Patil (University of Toledo),
X. Zhou (University of Toledo)
T. Z. Liu (University of Toledo)

D. Gall (Rennsselaer Polytechnic Institute)
B. R. Tuttle (Penn State University)
J. K. Bording (Brookhaven National Laboratory)
S. Kodambaka (University of California, LA)

Acknowledgements and Support

- **Funding**
  - U. of Toledo; NSF, Civil, Mechanical, and Manufacturing Innovation, Designing Materials to Revolutionize and Engineer our Future
  - DARPA
  - Wright Patterson Air Force Base

- **Computing**
  - NSF-MRI cluster at Toledo
  - Ohio Supercomputer Cluster
  - University of Toledo Parallel Computing Cluster
  - National Center for Supercomputing Applications (NCSA)

- **People**
  - Rick Irving

Outline

- General Introduction
- Experimental motivation for PtN
- PtN structure determination narrative
- Other Transition Metal nitrides
- Structural, mechanical and electronic properties
  - Lattice Constants
  - Bulk and shear moduli
  - Bulk modulus vs VED
  - LDOS
- Conclusions

Motivation for TM nitrides

Materials applications interest

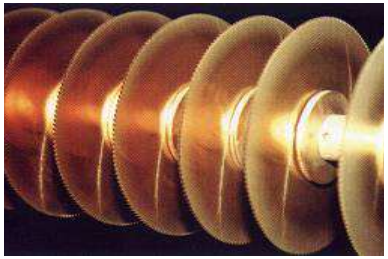

hard coatings

optics

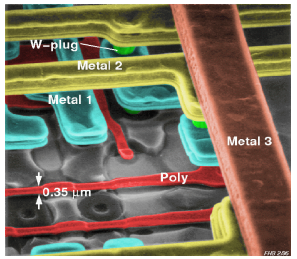

micro-electronics

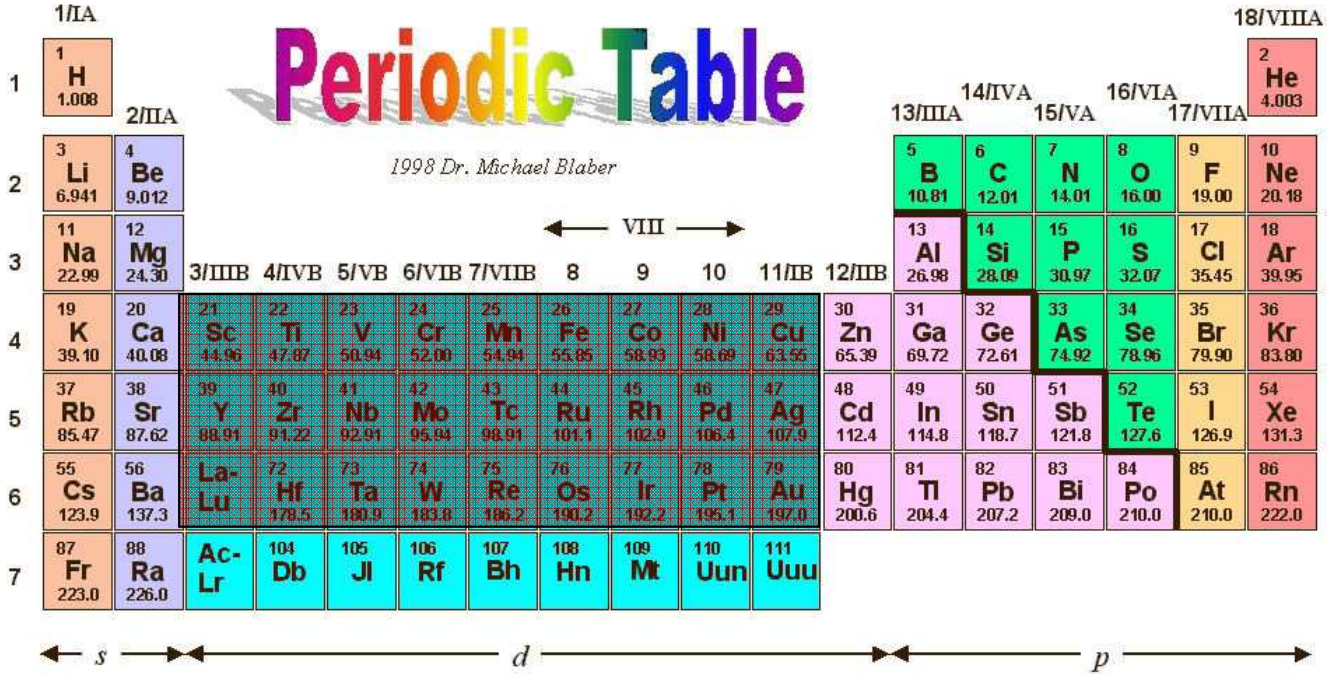

Small length scale 1 nm

Length scale: 1 nm
Materials: PtN and other nitrides
Phenomenon: Structural, mechanical, electronic properties
Techniques: Ab initio computations

Example

Length scale: 1 nm
Materials: PtN
Phenomenon: Structural, mechanical, electronic properties
Techniques: First principles computations DFT based
Motivation: Hard coating materials

Experimental synthesis of PtN

Experimental Synthesis and characterization of a binary noble metal nitride

E.Gregoryanz, C. Sanloup, M. Somayazulu, J. Badro, G. Giquet, H-K. Mao, and R. J. Hemley, Nat. Mat. 3, 294 (2004).

Although numerous metals react with nitrogen there are no known binary nitrides of the noble metals. We report the discovery and characterization of platinum nitride (PtN), the first binary nitride of the noble metals group.

This compound can be formed above 45–50 GPa and temperatures exceeding 2,000 K, and is stable after quenching to room pressure and temperature.

Synchrotron X-ray diffraction shows that the new phase is cubic with a remarkably high bulk modulus of 372(±5)GPa.

Structure of experimental PtN

Data is taken from two samples once with N as the pressure medium and once with He as the pressure medium.

All patterns at different pressure are consistent (see Fig. 3) and PtN can be indexed as f.c.c. (a = 4.8041(2) Å at 0.1 MPa) at all pressures.

Although the Rietveld refinement is complicated by the strong Pt signal, the refinement agrees with the non-centrosymmetric space group $F\bar{4}3m$,to which the zinc-blende structure belongs,as well as the rock-salt structure ($Fm\bar{3}m$); the large mass difference between Pt and N makes it impossible to distinguish between these two structures from the diffraction intensities.

The rock-salt structure does not have a first-order Raman spectrum and can therefore be ruled out. The zinc-blende structure has two Raman active peaks, consistent with the two strong first-order bands observed (see Fig. 1).

PtN stoichiometry and back-scattered electron image

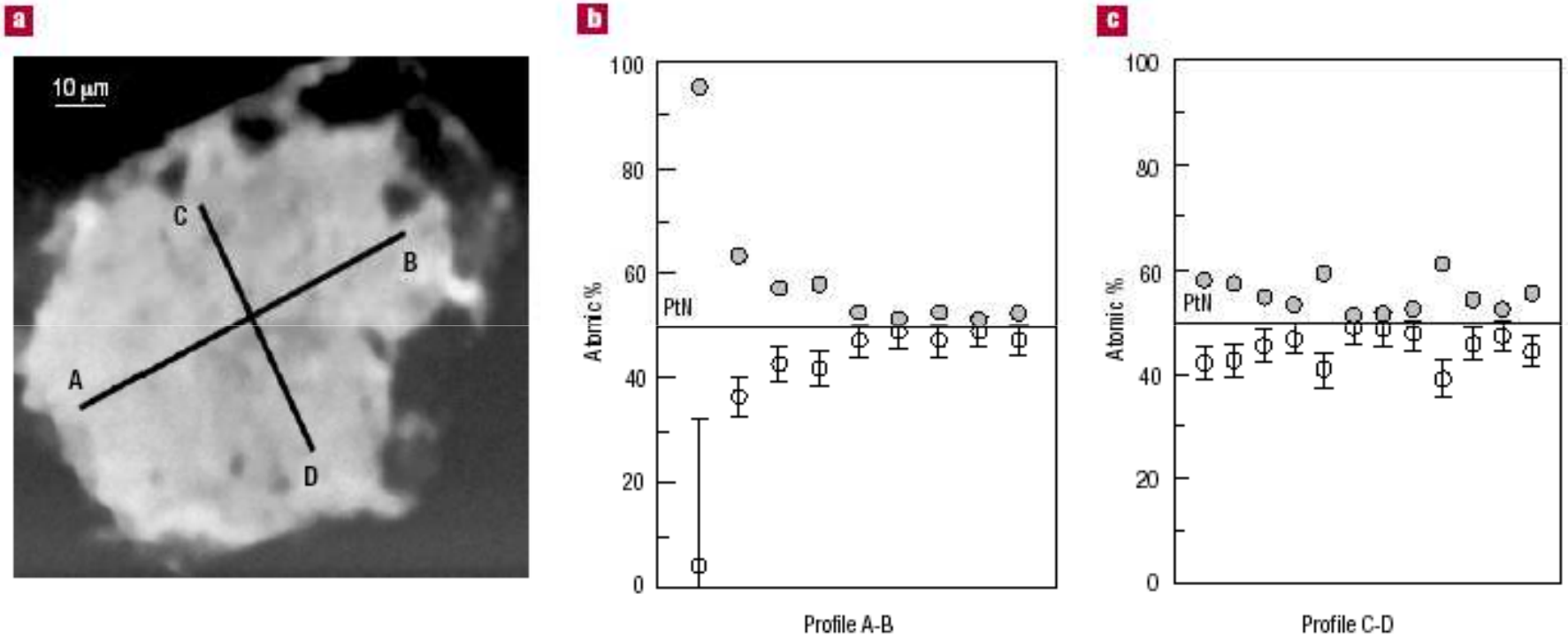

Figure 2 Chemical analysis of a reacted sample. **a**, Back-scattered electron image of an unloaded sample. **b**,**c**, Compositional profiles of the sample analysed by electron probe. Open circles: N content; closed circles: Pt content (the error bar on Pt is 0.55%).

Forms of PtN in our study

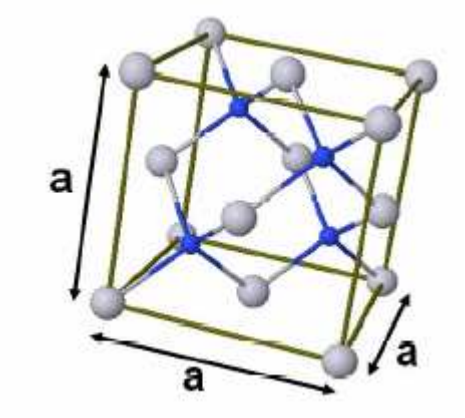

Zinc Blende

Rock Salt

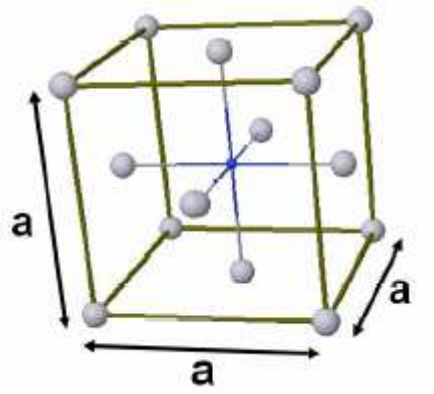

Pt:N ratio 1:1 in all forms

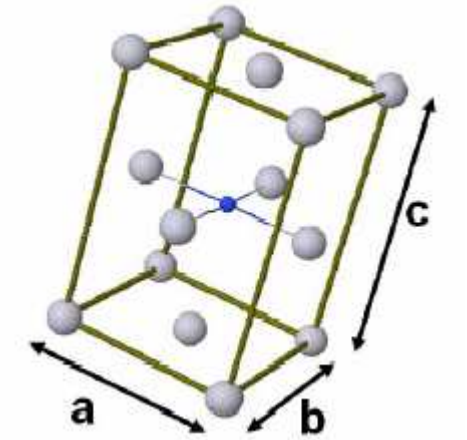

Face centered
Orthorhombic

Cooperite
(PtS form)

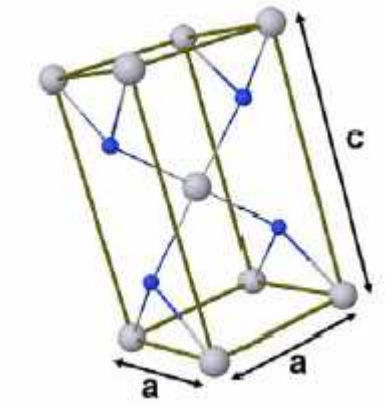

Lattice constants for zb and rs forms of PtN

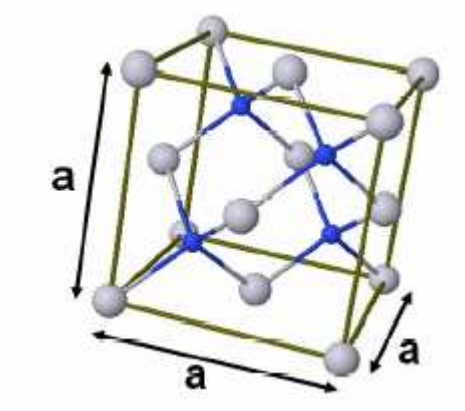

Theory with VASP

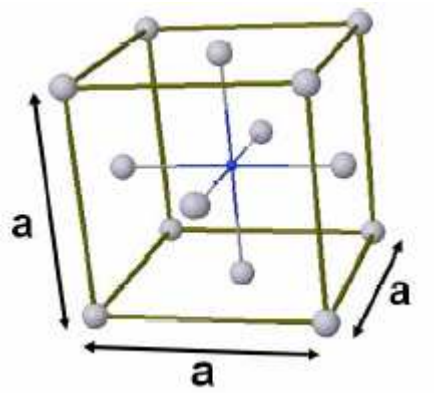

Zinc Blende

a = 0.4699 nm (LDA)
0.4781 nm (GGA)
B = 230 GPa (LDA)
192 GPa (GGA)

Rock Salt

a = 0.4407 nm (LDA)
0.4504 nm (GGA)
B = 284 GPa (LDA)
226 GPa (GGA)

Experiment, Gregoryanz et al. Nat. Mat. 3, 294 (2004)
a = 0.4801nm
B = 372 GPa

No effect of N vacancies on bulk modulus of PtN

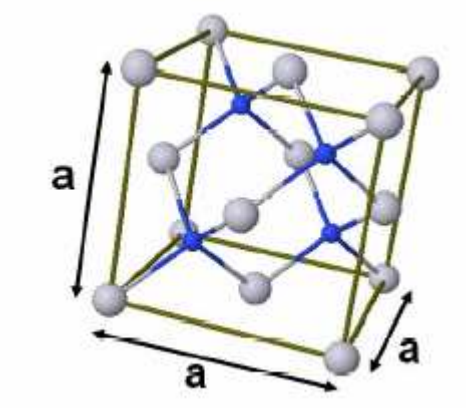

Zinc Blende

Theory with VASP

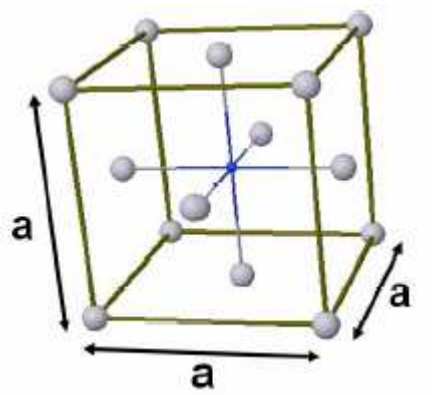

Rock Salt

No significant change in bulk modulus was found by introducing vacancies. We used Pt_1N_{1-x}, where x = 0, 0.037, and 0.125. Use 2 x 2 x 2 or 3 x 3x 3 fcc supercells.

In experiment, of Gregoryanz et al. Nat. Mat. 3, 294 (2004)

$0 < x < 0.05$

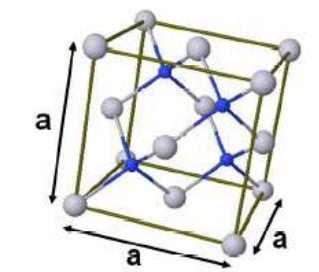

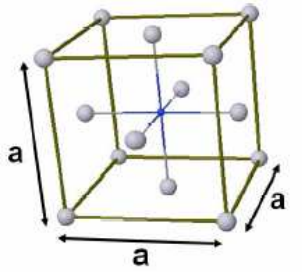

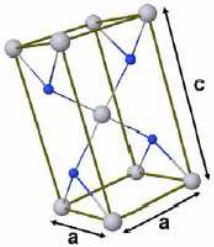

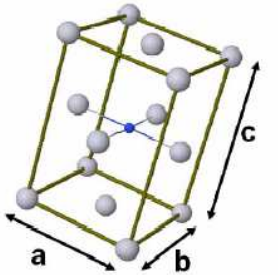

Elastic constants in GPa and stability

C_{ij} (in GPa)	Zinc blende	Rocksalt*	Cooperite	FCO
C_{11}	**210**	355	unstable	570
C_{22}	C_{11}	C_{11}	C_{11}	254
C_{33}	C_{11}	C_{11}	unstable	258
C_{44}	14	36	unstable	unstable
C_{55}	C_{44}	C_{44}	C_{44}	98
C_{66}	C_{44}	C_{44}	unstable	98
C_{12}	**241**	248	unstable	240
C_{13}	C_{12}	C_{12}	unstable	240
C_{23}	C_{12}	C_{12}	C_{13}	194

If $C_{11} - C_{12} < 0$ ==> unstable form. Also, any $C_{ij} < 0$ ==> unstable form. Also other conditions.

***Only stable form is rock salt.**

Elastic constants

Earlier theoretical work on PtN

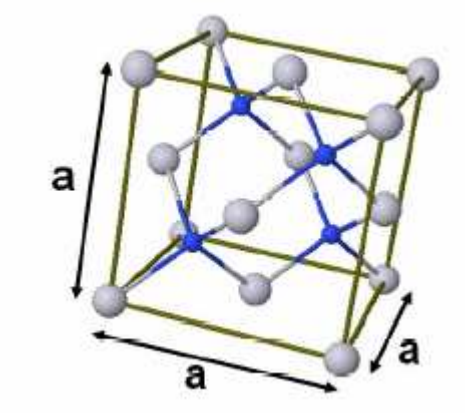

Theory with WIEN2K,
PRB 71, R041101 (2005).

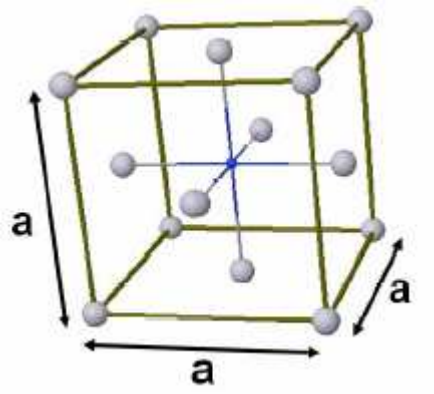

Zinc Blende

a = 0.4804 nm (GGA)
B = 371 GPa (GGA)

Rock Salt

a = 0.4518 nm (GGA)
B = 431 GPa (GGA)

Experiment, Gregoryanz et al. Nat. Mat. 3, 294 (2004)
a = 0.4801nm
B = 372 GPa

Theory matches perfectly with experiment!

Our manuscript would have read like this

We have done first principles calculations for the newly reported noble metal nitride PtN.

Our calculations contradict experimental findings published in *Nature Materials* by a well known group.

Our calculations also contradict theoretical findings by another well known theoretical group published in *PRB Rap. Comms*.

Results of both groups are in complete agreement with each other.

We think they are both wrong. We think we are right. Please accept this manuscript for publication.

More of earlier theoretical results for PtN

Lattice Structure	Present Work				Ref. [9]		Ref. [8]
	LDA		GGA		LDA	GGA	GGA
	VASP	WIEN2K	VASP	WIEN2K	WIEN2K	WIEN2K	WIEN2K
zb-PtN							
Bulk modulus (GPa)	**230**	235	**192**	178	**244**	**194**	371
Lattice constant (nm)	0.4699	0.4683	0.4794	0.4781	0.4692	0.4780	0.4804
$E_{f\text{-}r\text{-}t}$ (eV)	0.42						
rs-PtN							
Bulk modulus (GPa)	284	298	226	233	-	-	431
Lattice constant (nm)	0.4407	0.4397	0.4504	0.4496	-	-	0.4518
$E_{f\text{-}r\text{-}t}$ (eV)	0.75						

Experiment, Gregoryanz et al. Nat. Mat. 3, 294 (2004)
a = 0.4801nm and B = 372 GPa

[8] Phys. Rev. B 71, R041101 (2005).
[9] R. Yu and X. F. Zhang, Appl. Phys. Lett. 86, 121913 (2005).

Summary of theoretical results for PtN

Lattice Structure	Present Work				Ref. [9]		Ref. [8]
	LDA		GGA		LDA	GGA	GGA
	VASP	WIEN2K	VASP	WIEN2K	WIEN2K	WIEN2K	WIEN2K
zb-PtN							
Bulk modulus (GPa)	230	235	192	178	244	194	371
Lattice constant (nm)	0.4699	0.4683	0.4794	0.4781	0.4692	0.4780	0.4804
$E_{f\text{-}t}$ (eV)	0.42						
rs-PtN							
Bulk modulus (GPa)	284	298	226	233	-	-	431
Lattice constant (nm)	0.4407	0.4397	0.4504	0.4496	-	-	0.4518
$E_{f\text{-}t}$ (eV)	0.75						
fco-PtN							
Bulk modulus (GPa)	270						
Lattice constant (nm)	a = 0.3972 b = 0.3977 c = 0.6022						
$E_{f\text{-}t}$ (eV)	0.17						
co-PtN							
Bulk modulus (GPa)	-						
Lattice constant (nm)	a = 0.3323 b = a c = 0.4579						
$E_{f\text{-}t}$ (eV)	0						

Some evolution of the other theory

From: Erratum PRB 72, 119901 (E) (2005).

“We made a mistake of a factor of 2 in the unit cell volume while calculating the bulk modulus for the zinc-blende and rocksalt structure of PtN……..We thank Sanjay Khare and Chang-Zeng Fan for suggesting to us that we had miscalculated the bulk modulus.”

Conclusions of work on PtN

1. Zinc blende structure for PtN as claimed in experiment and an earlier theory is incorrect.

2. There exists a stable form of PtN the rock salt phase. It is not superhard.
   Has B < 300 GPa. Its lattice constant is around 0.44 nm.

3. The experimental form of PtN remains unknown.

4. Published theory and experiment can match each other and both be self-consistently wrong!

"Mechanical stability of possible structures of PtN investigated using first-principles calculations," S. K. R. Patil, S. V. Khare, B. R. Tuttle, J. K. Bording, and S. Kodambaka, *Phys. Rev. B* 73, 104118 (2006).

Experimental developments on PtN_2

- J. C. Crowhurst *et al*., Science 311, 1275 (2006). PtN is not PtN but is PtN_2, with pyrite structure.

MN_2, M = transition metal (Os, Ir, Pt, Au) (Experimental Observations)

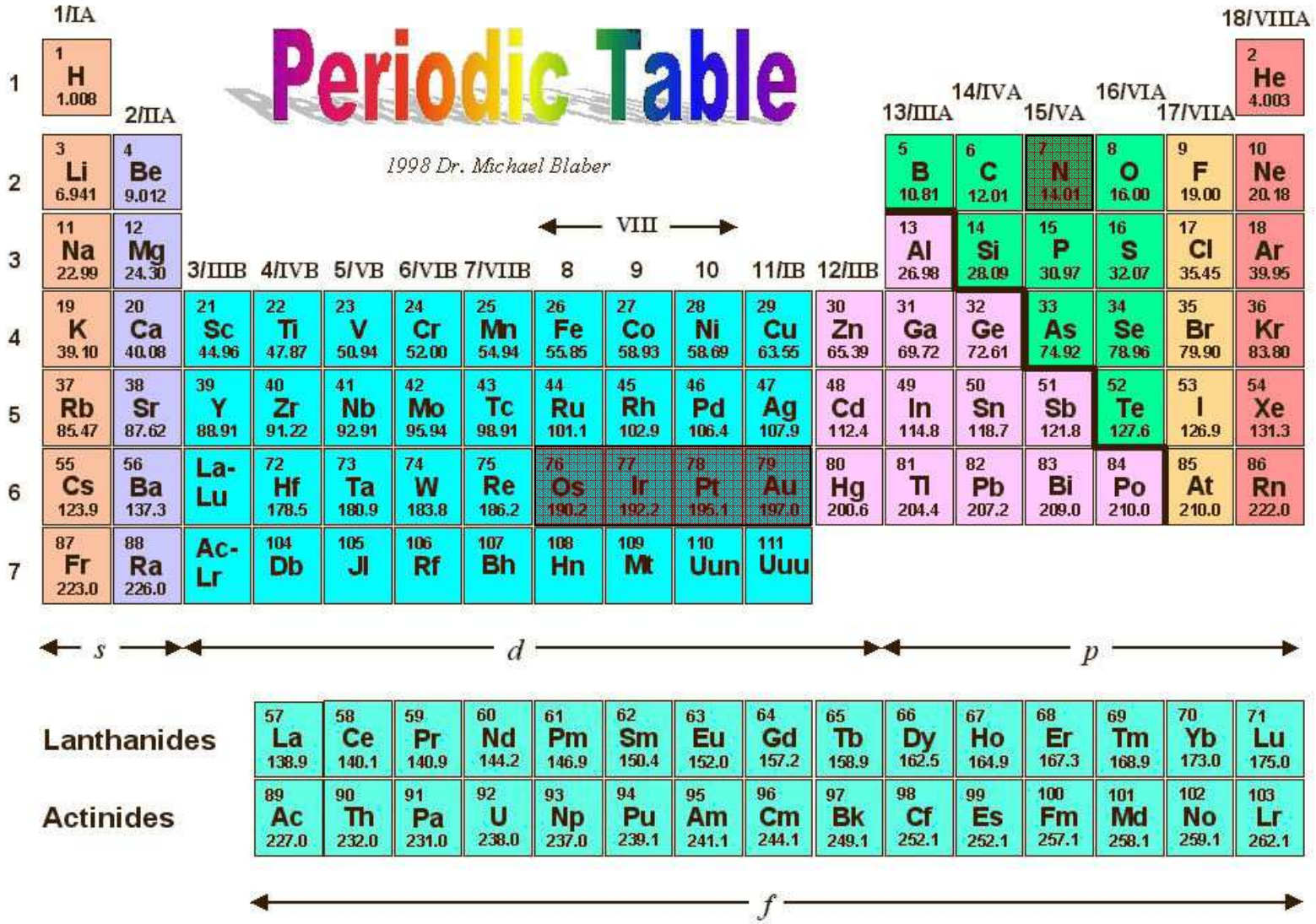

Motivation: New noble metal nitrides produced

Experiments

- PtN_2, (J. C. Crowhurst *et al*., Science 311, 1275 (2006).)
- IrN_2, OsN_2 (A. F. Young *et al*., Phys. Rev. Lett. 96, 155501 (2006).)

Computations

- IrN_2, OsN_2 (A. F. Young *et al*., Phys. Rev. Lett. 96, 155501 (2006).)
- PtN_2, (R. Yu *et al.,* Appl. Phys. Lett. 88, 51913 (2006).)
- PtN_2, (J. C. Crowhurst *et al*., Science 311, 1275 (2006).)
- PtN, (S. K. R. Patil *et al.,* Phys. Rev. B 73, 104118 (2006).)

Results

- Made in diamond anvil cells at 2000K and P = 50 GPa. Recovered at 300K and 0.1 MPa, ambient conditions.
- PtN_2 is now confirmed to be in pyrite phase.
- IrN_2, (hexagonal symmetry) and OsN_2 (orthorhombic symmetry) structures not fully confirmed.
- No thin film production method discovered!

Transition-metal nitrides: applications

Hard wear-resistant coatings
(TiN, ZrN, CrN, TaN)

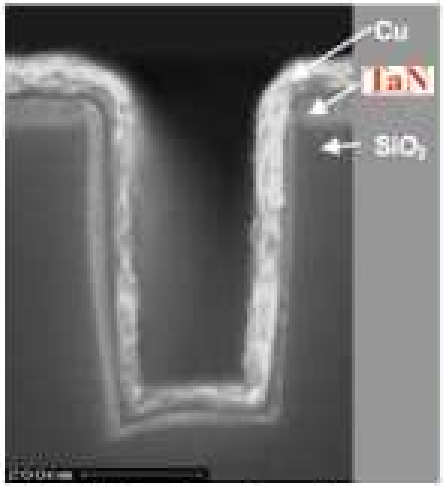

Diffusion barriers
(TiN, TaN)

Optical coatings
(TiN, ZrN)

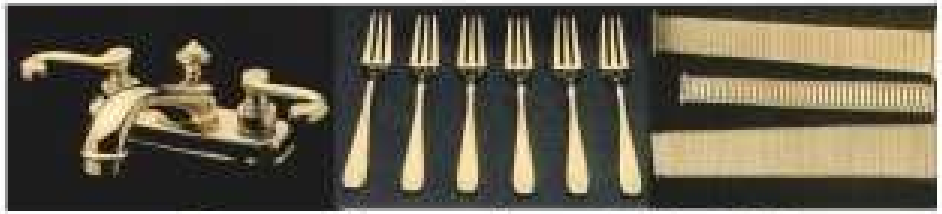

Decorative coatings (TiN, ZrN)

Buy Now & Save!

3 PC. LOT NO. 91616/8873

TITANIUM NITRIDE COATED M2 HIGH SPEED STEEL STEP DRILLS

Includes (A) 3/16" to 1/2" six step bit, (B) 1/4" to 3/4" nine step bit and (C) 1/8" to 1/2" thirteen step bit.

DRILL MASTER

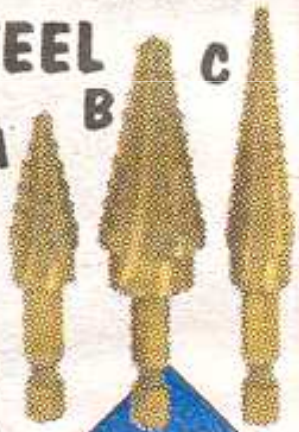

Item 8873 shown

$14.99

REGULAR PRICE $29.99

SAVE 50%

Transition Metal Nitrides (TMNs)

- Refractory hard materials
- Extremely high hardness – wear resistance
- High melting points – thermal resistance
- Good electrical and thermal conductivity
- Good corrosion or oxidation resistance

Evolutionary Development of Nitride Hard Coatings

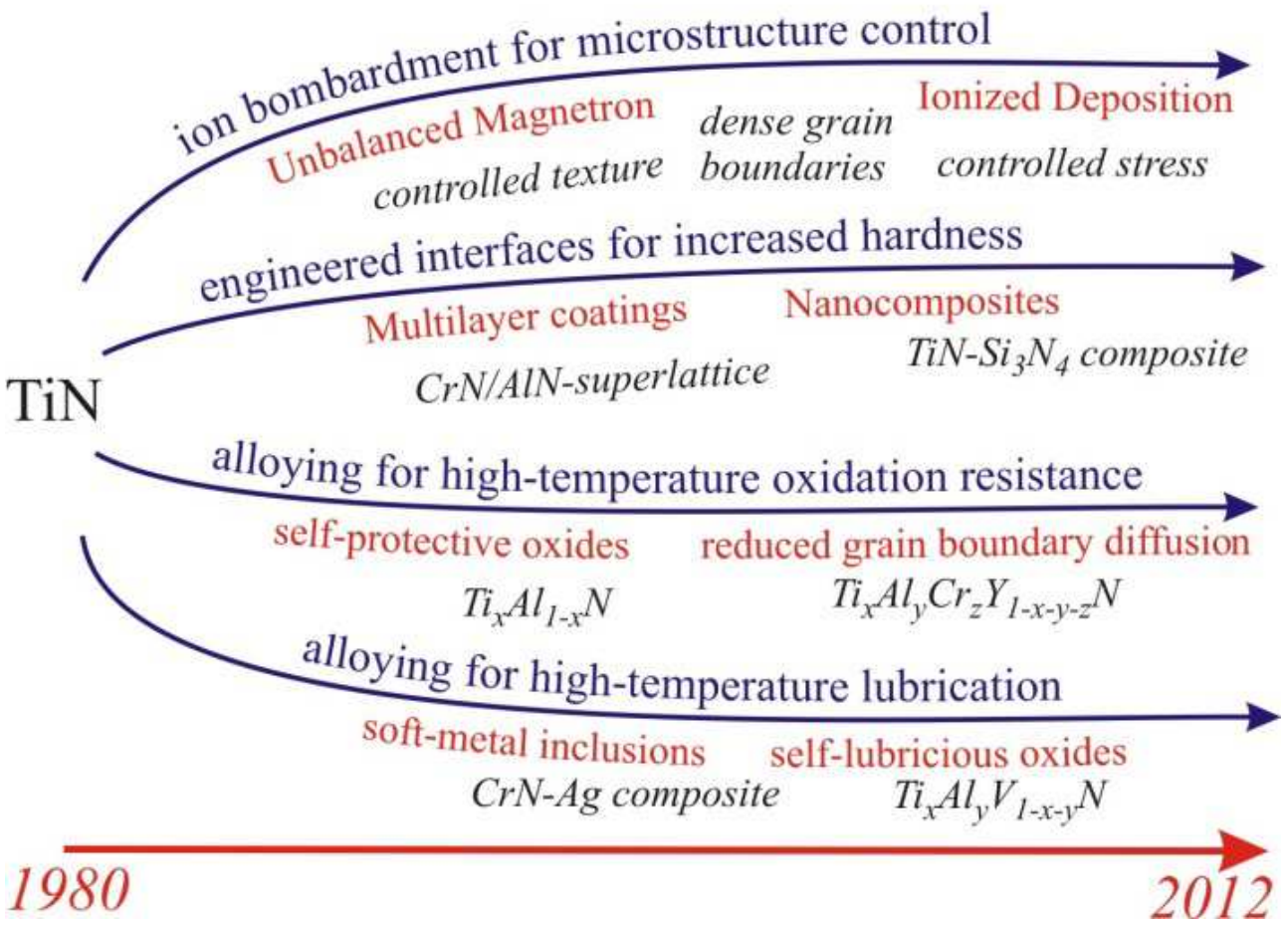

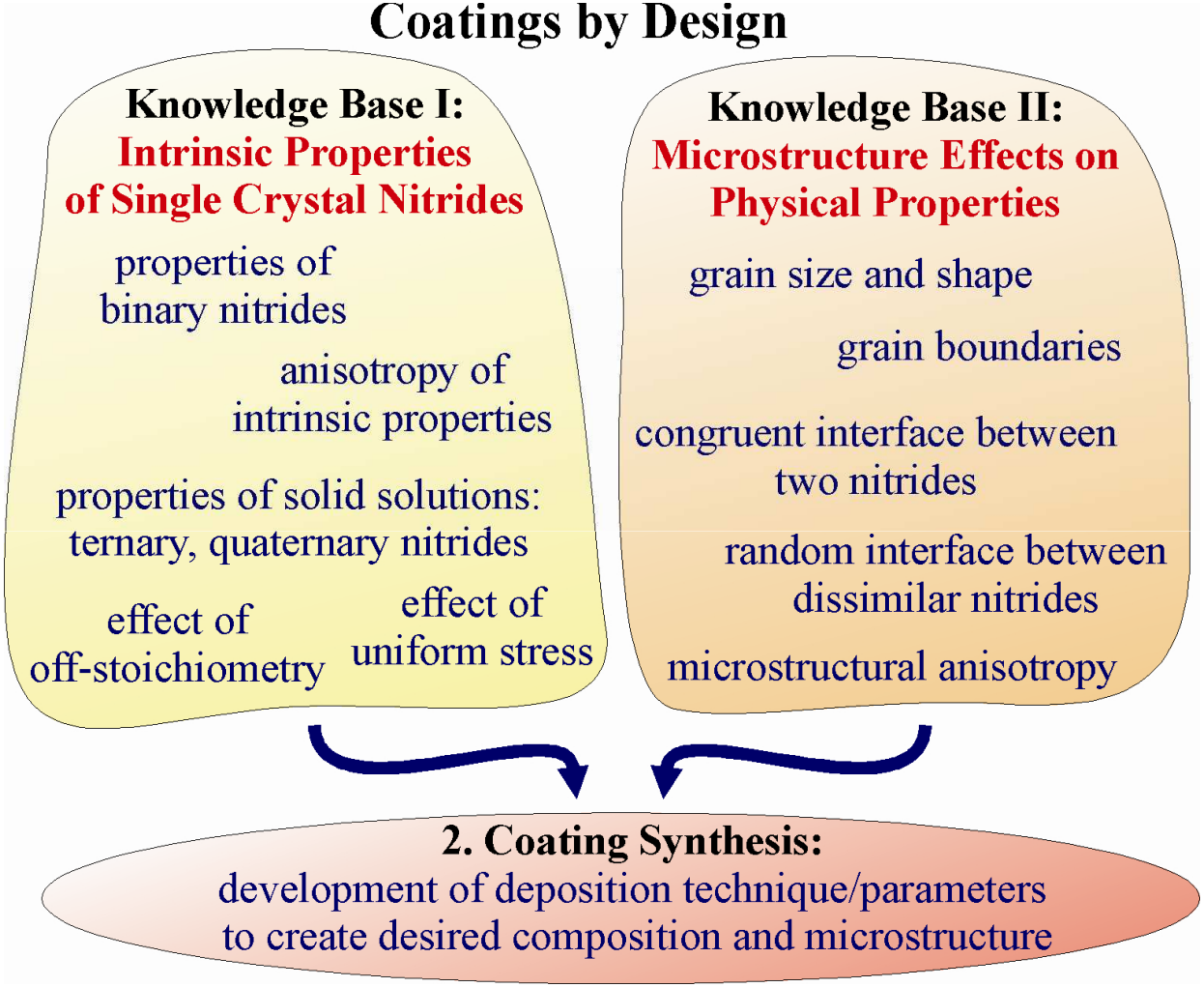
Coatings by Design
Knowledge Base I:
Intrinsic Properties
of Single Crystal Nitrides
properties of
binary nitrides
anisotropy of
intrinsic properties
properties of solid solutions:
ternary, quaternary nitrides
effect of
off-stoichiometry
effect of
uniform stress
Knowledge Base II:
Microstructure Effects on
Physical Properties
grain size and shape
grain boundaries
congruent interface between
two nitrides
random interface between
dissimilar nitrides
microstructural anisotropy
2. Coating Synthesis:
development of deposition technique/parameters
to create desired composition and microstructure

The General Program

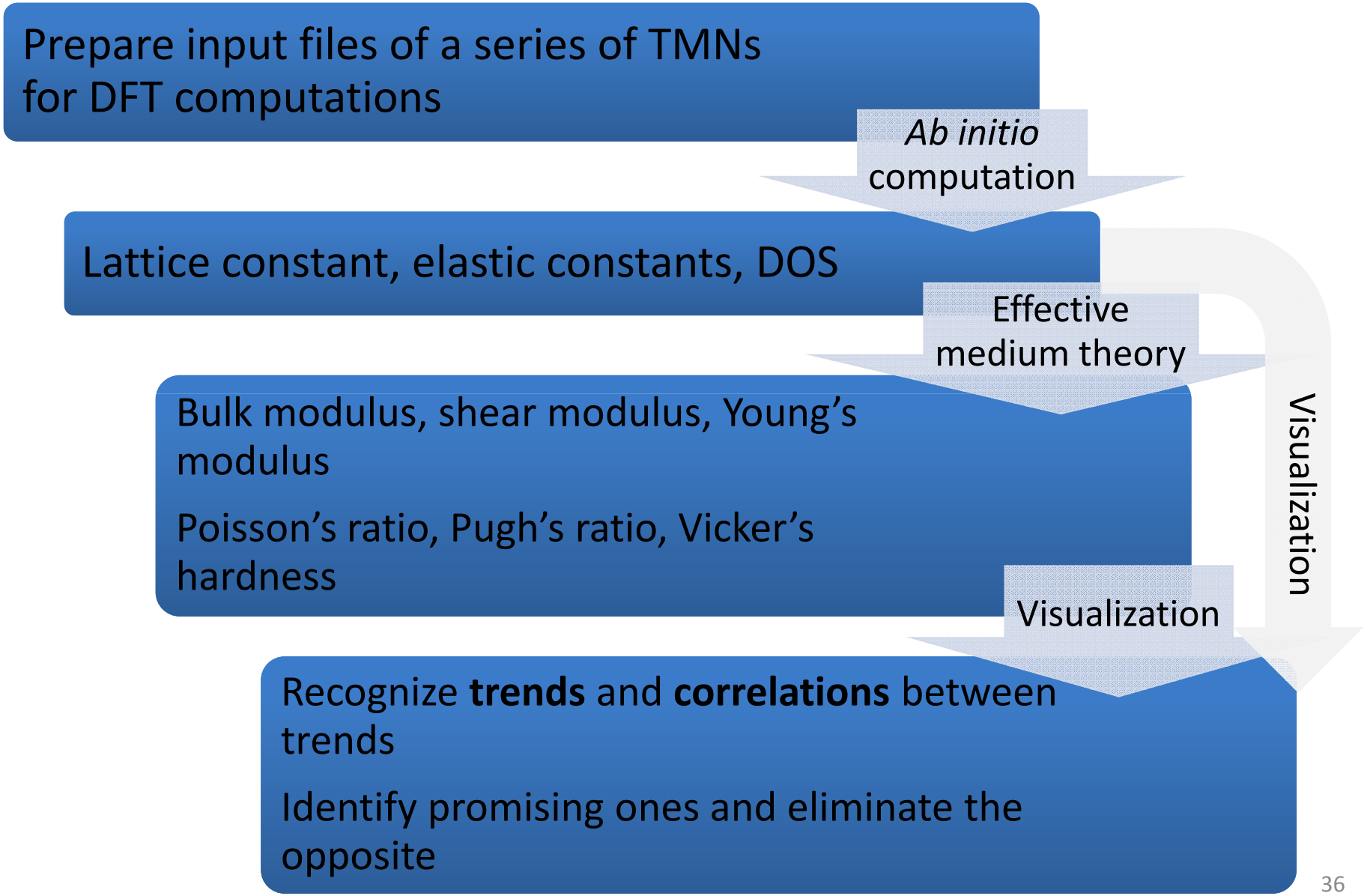

Applicability of *Ab Initio* Methods

Pros

Very good at predicting structural properties:

(1) Lattice constant good to 1-3%

(2) Elastic constants good to 1-10%

(3) Very robust relative energy ordering between structures

(4) Good pressure induced phase changes

Good band structures, electronic properties

Good phonon spectra

Good chemical reaction and bonding pathways

Cons

Computationally intensive

Band gaps are wrong

Excited electronic states are difficult

Motivation for MN_2 based compounds

M = Hf, Ta, W, Re, Os, Ir, Pt, Au

Our theoretical computations; Cubic phases:

Pyrite, Fluorite, Zinc blende, Rocksalt

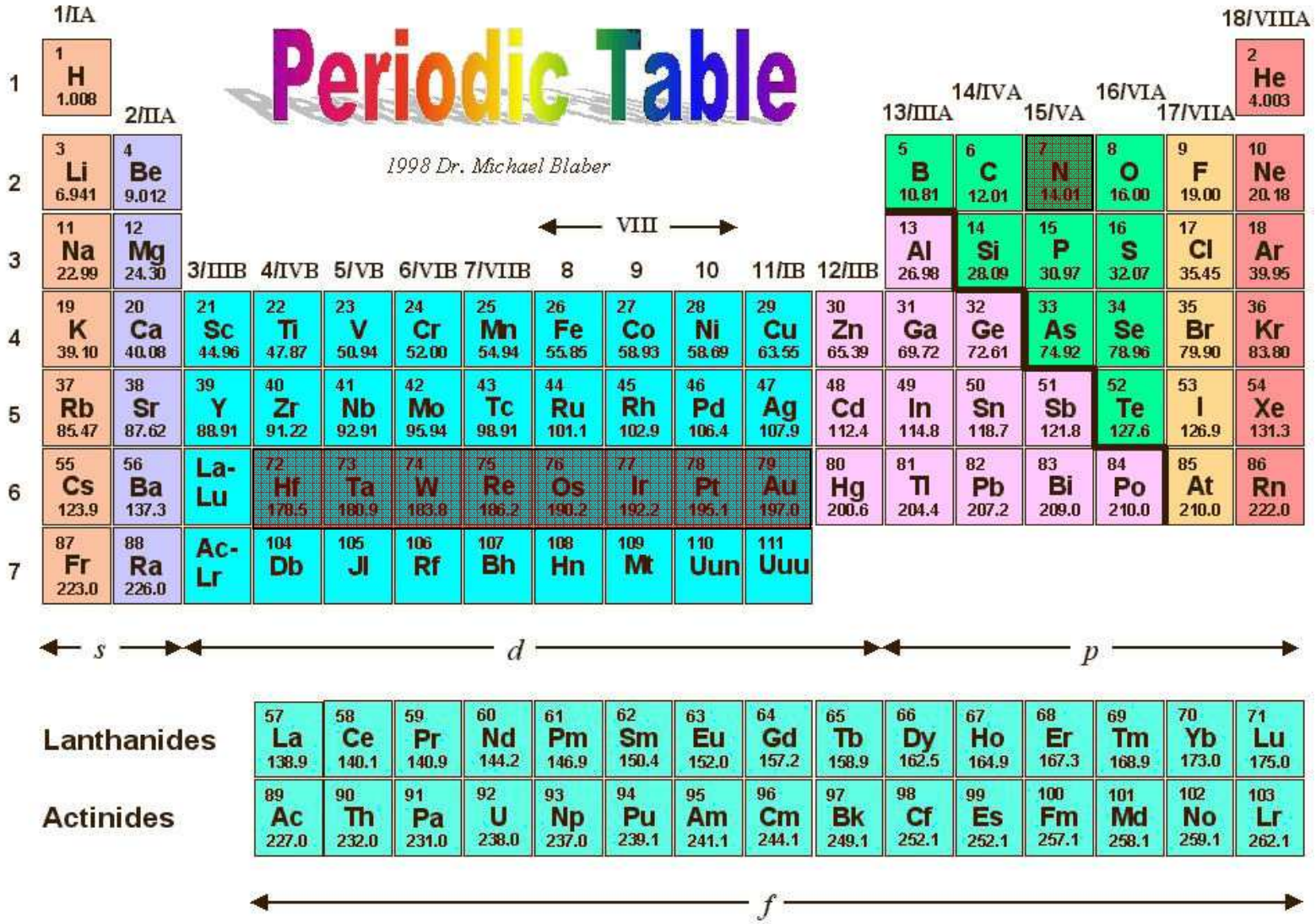

Fluorite(C1) Phase [MN_2]

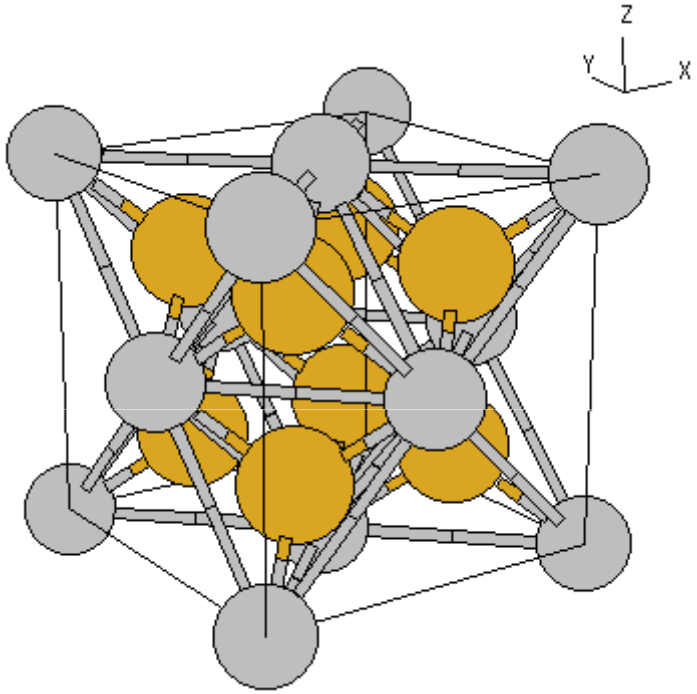

Lattice Vectors

$\mathbf{A}_1 = \frac{1}{2}\,a\,\mathbf{Y} + \frac{1}{2}\,a\,\mathbf{Z}$

$\mathbf{A}_2 = \frac{1}{2}\,a\,\mathbf{X} + \frac{1}{2}\,a\,\mathbf{Z}$

$\mathbf{A}_3 = \frac{1}{2}\,a\,\mathbf{X} + \frac{1}{2}\,a\,\mathbf{Y}$

Basis Vectors

$\mathbf{B}_1 = 0$

$\mathbf{B}_2 = +\frac{1}{4}\mathbf{A}_1 + \frac{1}{4}\mathbf{A}_2 + \frac{1}{4}\mathbf{A}_3 = +\frac{1}{4}\,a\,\mathbf{X} + \frac{1}{4}\,a\,\mathbf{Y} + \frac{1}{4}\,a\,\mathbf{Z}$

$\mathbf{B}_3 = -\frac{1}{4}\mathbf{A}_1 - \frac{1}{4}\mathbf{A}_2 - \frac{1}{4}\mathbf{A}_3 = -\frac{1}{4}\,a\,\mathbf{X} - \frac{1}{4}\,a\,\mathbf{Y} - \frac{1}{4}\,a\,\mathbf{Z}$

Metal

Nitrogen

Pyrite (C2) Phase [MN_2]

Lattice Vectors

$\mathbf{A}_1 = a\,\mathbf{X}$

$\mathbf{A}_2 = a\,\mathbf{Y}$

$\mathbf{A}_3 = a\,\mathbf{Z}$

Basis Vectors

$\mathbf{B}_1$	=	0		
$\mathbf{B}_2$	=	$\frac{1}{2}\mathbf{A}_2 + \frac{1}{2}\mathbf{A}_3$	=	$\frac{1}{2}a\,\mathbf{Y} + \frac{1}{2}a\,\mathbf{Z}$
$\mathbf{B}_3$	=	$\frac{1}{2}\mathbf{A}_1 + \frac{1}{2}\mathbf{A}_3$	=	$\frac{1}{2}a\,\mathbf{X} + \frac{1}{2}a\,\mathbf{Z}$
$\mathbf{B}_4$	=	$\frac{1}{2}\mathbf{A}_1 + \frac{1}{2}\mathbf{A}_2$	=	$\frac{1}{2}a\,\mathbf{X} + \frac{1}{2}a\,\mathbf{Y}$
$\mathbf{B}_5$	=	$u\,\mathbf{A}_1 + u\,\mathbf{A}_2 + u\,\mathbf{A}_3$	=	$u\,a\,\mathbf{X} + u\,a\,\mathbf{Y} + u\,a\,\mathbf{Z}$
$\mathbf{B}_6$	=	$-u\,\mathbf{A}_1 - u\,\mathbf{A}_2 - u\,\mathbf{A}_3$	=	$-u\,a\,\mathbf{X} - u\,a\,\mathbf{Y} - u\,a\,\mathbf{Z}$
$\mathbf{B}_7$	=	$(\frac{1}{2}+u)\,\mathbf{A}_1 + (\frac{1}{2}-u)\,\mathbf{A}_2 - u\,\mathbf{A}_3$	=	$(\frac{1}{2}+u)\,a\,\mathbf{X} + (\frac{1}{2}-u)\,a\,\mathbf{Y} - u\,a\,\mathbf{Z}$
$\mathbf{B}_8$	=	$-(\frac{1}{2}+u)\,\mathbf{A}_1 - (\frac{1}{2}-u)\,\mathbf{A}_2 + u\,\mathbf{A}_3$	=	$-(\frac{1}{2}+u)\,a\,\mathbf{X} - (\frac{1}{2}-u)\,a\,\mathbf{Y} + u\,a\,\mathbf{Z}$
$\mathbf{B}_9$	=	$-u\,\mathbf{A}_1 + (\frac{1}{2}+u)\,\mathbf{A}_2 + (\frac{1}{2}-u)\,\mathbf{A}_3$	=	$-u\,a\,\mathbf{X} + (\frac{1}{2}+u)\,a\,\mathbf{Y} + (\frac{1}{2}-u)\,a\,\mathbf{Z}$
$\mathbf{B}_{10}$	=	$u\,\mathbf{A}_1 - (\frac{1}{2}+u)\,\mathbf{A}_2 - (\frac{1}{2}-u)\,\mathbf{A}_3$	=	$u\,a\,\mathbf{X} - (\frac{1}{2}+u)\,a\,\mathbf{Y} - (\frac{1}{2}-u)\,a\,\mathbf{Z}$
$\mathbf{B}_{11}$	=	$(\frac{1}{2}-u)\,\mathbf{A}_1 - u\,\mathbf{A}_2 + (\frac{1}{2}+u)\,\mathbf{A}_3$	=	$(\frac{1}{2}-u)\,a\,\mathbf{X} - u\,a\,\mathbf{Z} + (\frac{1}{2}+u)\,a\,\mathbf{Z}$
$\mathbf{B}_{12}$	=	$-(\frac{1}{2}-u)\,\mathbf{A}_1 + u\,\mathbf{A}_2 - (\frac{1}{2}+u)\,\mathbf{A}_3$	=	$-(\frac{1}{2}-u)\,a\,\mathbf{X} + u\,a\,\mathbf{Z} - (\frac{1}{2}+u)\,a\,\mathbf{Z}$

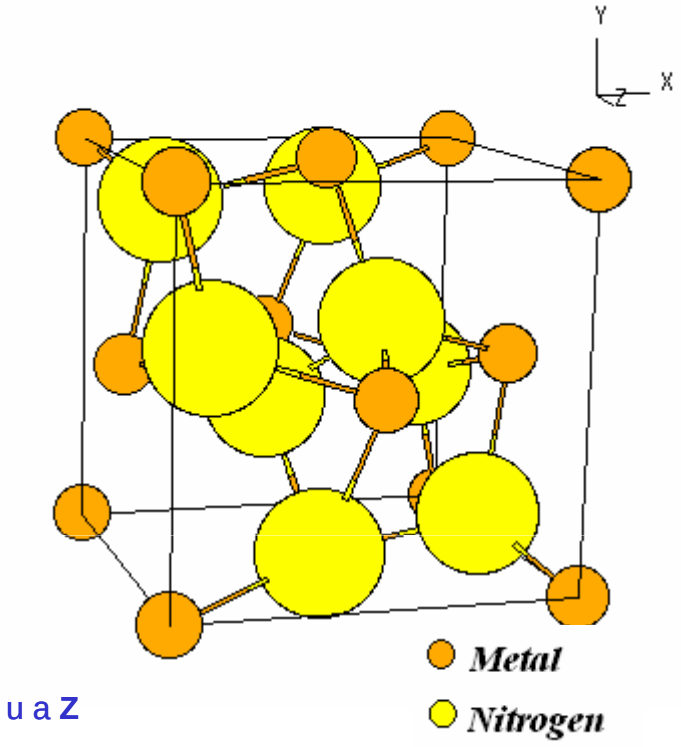

Zincblende(B3) Phase [MN]

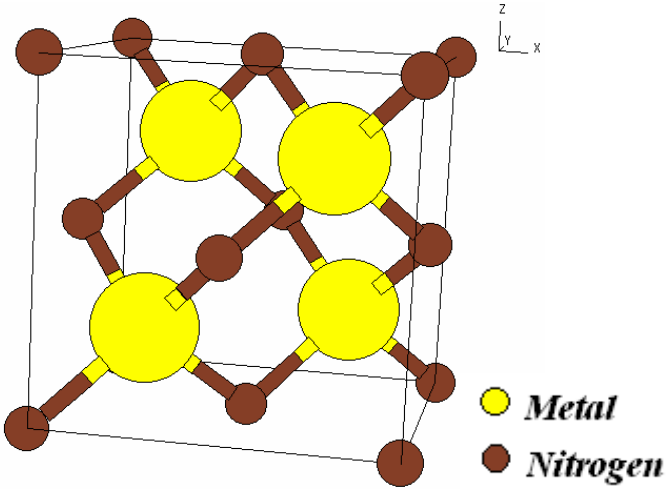

Lattice Vectors

$\mathbf{A_1} = \frac{1}{2}a\,\mathbf{Y} + \frac{1}{2}a\,\mathbf{Z}$

$\mathbf{A_2} = \frac{1}{2}a\,\mathbf{X} + \frac{1}{2}a\,\mathbf{Z}$

$\mathbf{A_3} = \frac{1}{2}a\,\mathbf{X} + \frac{1}{2}a\,\mathbf{Y}$

Basis Vectors

$\mathbf{B_1} = 0$

$\mathbf{B_2} = \frac{1}{4}\mathbf{A_1} + \frac{1}{4}\mathbf{A_2} + \frac{1}{4}\mathbf{A_3} = \frac{1}{4}a\,\mathbf{X} + \frac{1}{4}a\,\mathbf{Y} + \frac{1}{4}a\mathbf{Z}$

Rocksalt(B1) Phase [MN]

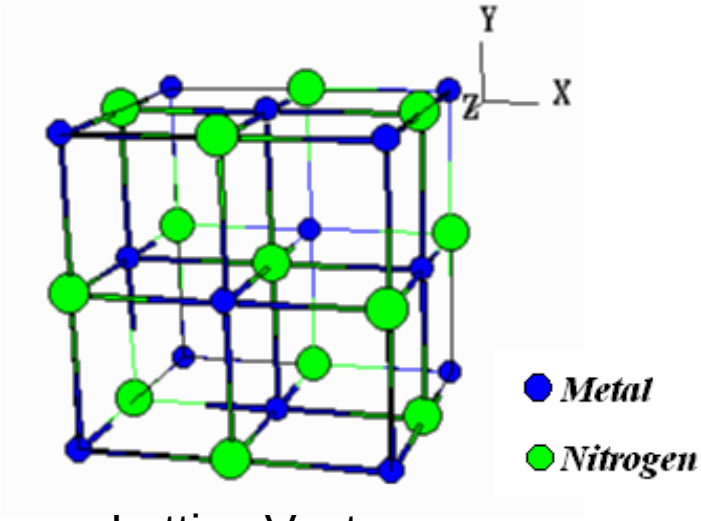

Lattice Vectors

$\mathbf{A_1} = \frac{1}{2}a\,\mathbf{Y} + \frac{1}{2}a\,\mathbf{Z}$

$\mathbf{A_2} = \frac{1}{2}a\,\mathbf{X} + \frac{1}{2}a\,\mathbf{Z}$

$\mathbf{A_3} = \frac{1}{2}a\,\mathbf{X} + \frac{1}{2}a\,\mathbf{Y}$

Basis Vectors

$\mathbf{B_1} = 0$

$\mathbf{B_2} = \frac{1}{2}\mathbf{A_1} + \frac{1}{2}\mathbf{A_2} + \frac{1}{2}\mathbf{A_3} = \frac{1}{2}a\mathbf{X} + \frac{1}{2}a\mathbf{Y} + \frac{1}{2}a\mathbf{Z}$

Ab initio method details

- LDA, Ceperley-Alder exchange-correlation functional as parameterized by Perdew and Zunger
- Generalized ultra-soft Vanderbilt pseudo-potentials and plane wave basis set
- Supercell approach with periodic boundary conditions in all three dimensions
- Energy cut-offs of 300 eV, Monkhrost-Pack dense k-point meshes

Table I: Fluorite phases

MN_2	a (Å)	C_{11} (GPa)	C_{12} (GPa)	C_{44} (GPa)	B (GPa)	E (eV)
HfN_2	5.068	Unstable	Unstable	Unstable	251.1	Unstable
TaN_2	4.930	Unstable	Unstable	Unstable	323.8	Unstable
WN_2	4.855	Unstable	Unstable	Unstable	359.8	Unstable
ReN_2	4.820	426.0	345.3	36.0	372.2	-30.18
OsN_2	4.794 (4.781[a])	496.0 (544.5 [a])	313.2 (309.8 [a])	96.1 (103.9 [a])	374.1 (388.0 [a])	-28.36
IrN_2	4.815 (4.801[b])	459.7 (464.0[b])	306.9 (339.0 [b])	128.8 (124.0 [b])	357.8 (381.0 [b])	-25.67
PtN_2	4.886 (4.866 [b])	500.5 (532.0 [b])	199.2 (208.0 [b])	112.5 (122.0 [b])	299.7 (316.0 [b])	-21.99
AuN_2	5.068 (5.035 [b])	349.9 (371.0 [b])	179.2 (183.0 [b])	71.0 (71.0 [b])	236.1 (246.0 [b])	-16.50

All results with DFT-LDA

[a] R. Yu and X.F. Zhang, Phys. Rev. B 72 (2005) 054103.

[b] C.Z. Fan, S.Y. Zeng, L.X. Li, Z.J. Zhan, R.P. Liu, W.K. Wang, P. Zhang, Y.G. Yao, Phys. Rev B 74 (2006) 125118.

Table II: Pyrite phases

MN_2	a (Å)	C_{11} (GPa)	C_{12} (GPa)	C_{44} (GPa)	B (GPa)	E (eV)
HfN_2	5.029	305	222	64	250	-31.87
TaN_2	5.005	322	224	60	256	-31.79
WN_2	4.928	497	253	52	334	-31.75
ReN_2	4.880	521	261	80	348	-30.36
OsN_2	4.839 (4.925[a])	616 (523[a])	266 (213[a])	104 (107 [a])	383 (316 [a])	-28.68
IrN_2	4.781	804	147	79	366	-27.14
PtN_2	4.792	845 (824 [c])	101 (117 [c])	160 (152 [c])	349 (352 [c])	-24.69
AuN_2	5.005	453	343	61	380	-19.29

All results with DFT-LDA

[a] C.Z. Fan, S.Y. Zeng, L.X. Li, Z.J. Zhan, R.P. Liu, W.K. Wang, P. Zhang, Y.G. Yao, Phys. Rev B 74 (2006) 125118.

[c] R. Yu, Q. Zhan, and X. F. Zhang, Appl. Phys. Lett 88 (2006) 051913.

Table III: Zinc-blende and rocksalt phases

MN	a (Å)	C_{11} (GPa)	C_{12} (GPa)	C_{44} (GPa)	B (GPa)	E (eV)
HfN (zb)	4.796	326.1	166.5	107.7	219.7	-23.25
(rs)	4.436	704.9	111.8	131.0	309.5	-24.11
TaN (zb)	4.659	314.9	258.8	13.0	274.2	-23.82
(rs)	4.326	826.9	155.9	73.4	379.6	-24.47
IrN (zb)	4.573	316.2	275.8	55.8	289.3	-17.99
(rs)	4.328	Unstable	Unstable	Unstable	346.0	Unstable
PtN (zb)	4.699	Unstable	Unstable	Unstable	230.3	Unstable
(rs)	4.407	355.0	248.0	36.0	284	-24.10
AuN (zb)	4.870	Unstable	Unstable	Unstable	161.1	Unstable
(rs)	4.5648	312.5	169.4	28.8	217.1	-10.31

WN, ReN, OsN are unstable in both zinc-blende and rocksalt phases.

All results with DFT-LDA

Bulk (B) and shear (G) moduli of stable period VI transition metal nitrides

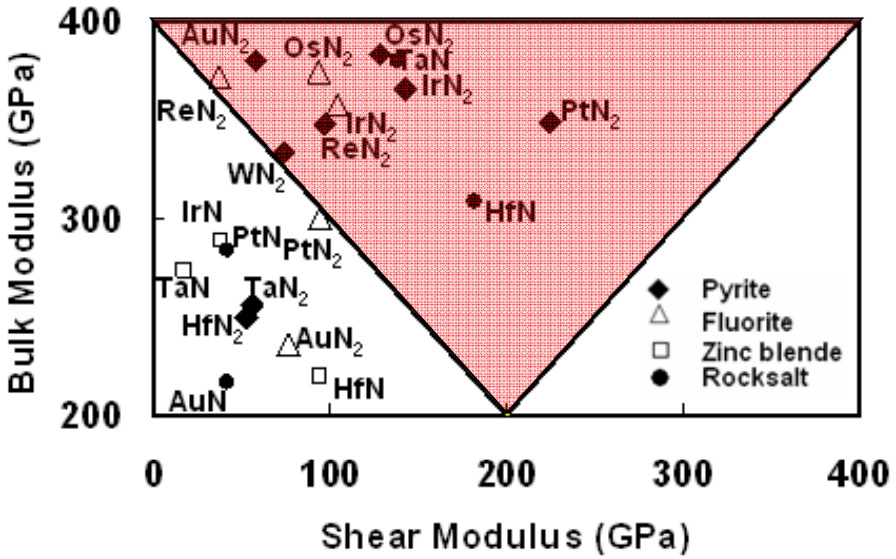

For hard coatings the material should be in the red triangle

B/G ratio > 1 implies more ductility
B/G ratio < 1 implies more hardness
(As hardness correlates better with shear modulus than bulk modulus),
L. R. Zhao *et al.,* Surf. Coat. Technol. 200, 1595 (2005).

Pyrite: **AuN_2, ReN_2, WN_2, OsN_2, IrN_2, PtN_2**, TaN_2, HfN_2
Fluorite: **ReN_2, OsN_2, IrN_2**, PtN_2, AuN_2
Zinc blende: IrN, TaN, HfN
Rocksalt: **TaN, HfN**, PtN, AuN

B vs VED for fluorite and pyrite phases of period VI transition metal nitrides

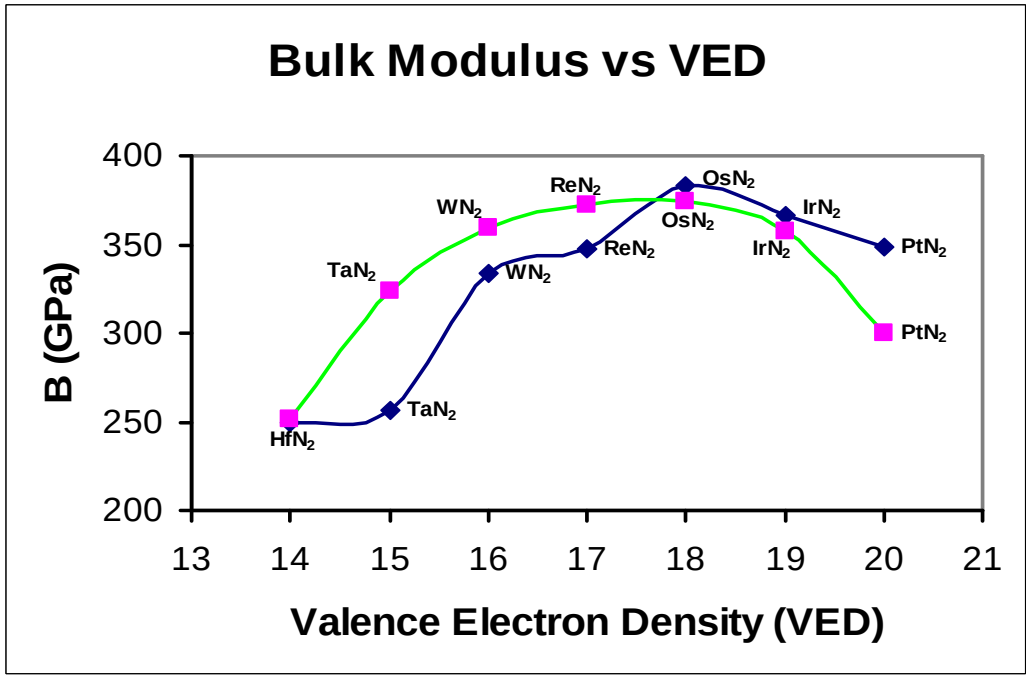

- Pyrite
- Fluorite

For fluorite and pyrite phases, VED increases in steps of unity from 14 for HfN_2 to 20 for PtN_2 as each extra electron is added to the d orbital.

In case of both fluorite and pyrite phases, B increases from HfN_2 to OsN_2 and decreases from OsN_2 to PtN_2. B peaks at OsN_2 with a VED of 18.

It may be speculated that 18 being a number associated with the valence shell configuration of the noble elements, which are chemically very stable, may have a causal relationship with the peaking of B values.

Local Density of States (LDOS)

Pyrite Phases

B_{Hf} = 250 GPa

B_{Ir} = 366 GPa

B_{Au} = 380 GPa

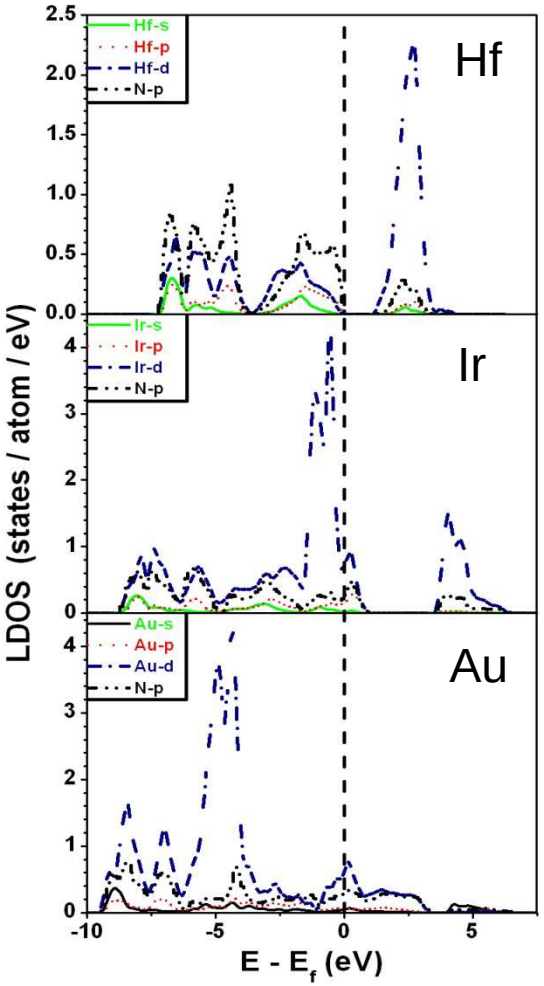

LDOS for pyrite phases of HfN_2, IrN_2, and AuN_2.

Pyrite vs Fluorite

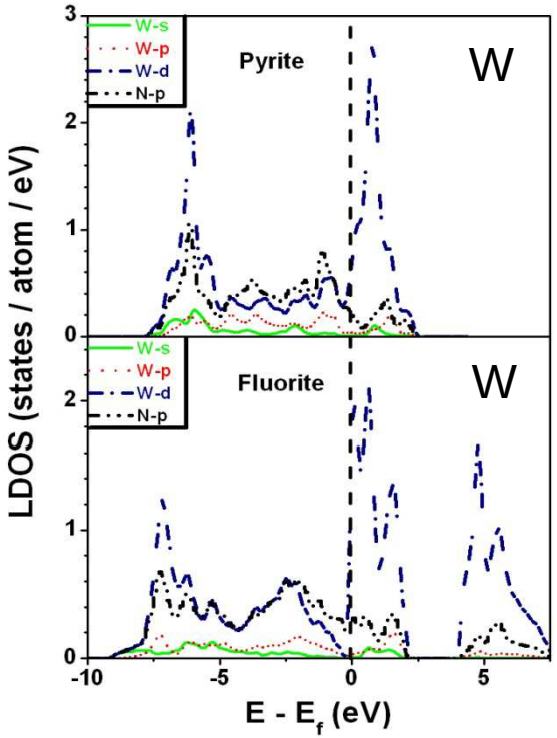

Pyrite Stable

Fluorite Unstable

LDOS of WN_2, in pyrite and fluorite phases.

Conclusions

[S.K.R. Patil, S.V. Khare *et al.,* Thin Solid Films, 517, 824 (2008).]

1. We studied 32 cubic phases of period VI transition metal nitrides.

2. ReN_2 in fluorite and pyrite phases and WN_2 in pyrite phase are mechanically stable with a high B. The high B is attributed to strong metal d and nitrogen p orbital hybridization.

3. We further tested the suitability in hard coating applications of this class of cubic transition metal nitrides (zinc-blende, rocksalt, fluorite, and pyrite phases).

4. The mechanical instability of the unstable phases is correlated with high DOS at Fermi level.

5. The bulk modulus for both pyrite and fluorite phases has a peak at a valence electron density of 18.

6. We hope that the present calculations would lead to the synthesis of hard WN_2 and ReN_2 and motivate the research of such crystal structures in the hard coatings industry.

Periodic Table 3d highlight

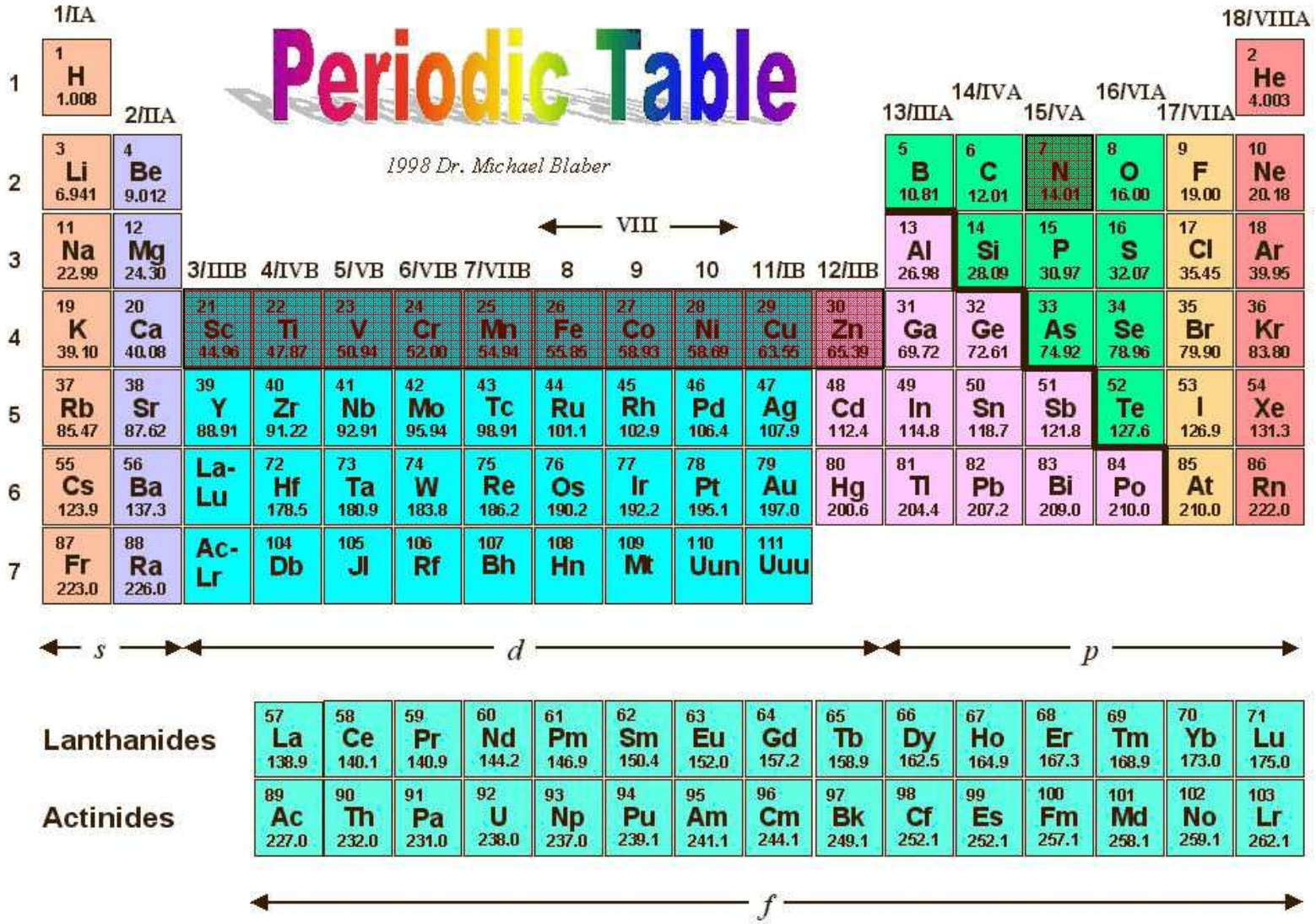

Structure – zincblende (MN)

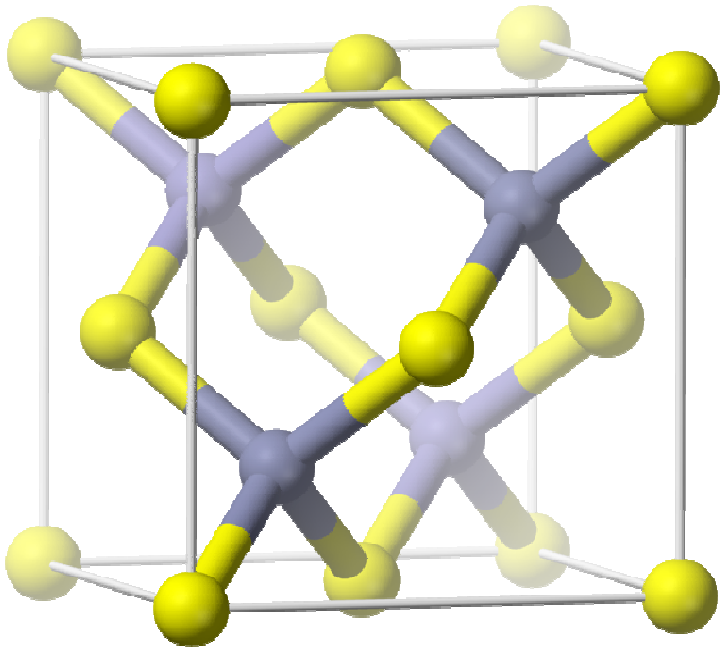

Lattice Vectors

$\mathbf{A}_1 = \frac{1}{2}\,a\,\mathbf{Y} + \frac{1}{2}\,a\,\mathbf{Z}$

$\mathbf{A}_2 = \frac{1}{2}\,a\,\mathbf{X} + \frac{1}{2}\,a\,\mathbf{Z}$

$\mathbf{A}_3 = \frac{1}{2}\,a\,\mathbf{X} + \frac{1}{2}\,a\,\mathbf{Y}$

Basis Vectors

$\mathbf{B}_1 = 0$

$\mathbf{B}_2 = \frac{1}{4}\,\mathbf{A}_1 + \frac{1}{4}\,\mathbf{A}_2 + \frac{1}{4}\,\mathbf{A}_3 = \frac{1}{4}\,a\,\mathbf{X} + \frac{1}{4}\,a\,\mathbf{Y} + \frac{1}{4}\,a\,\mathbf{Z}$

http://en.wikipedia.org/wiki/File:Sphalerite-unit-cell-depth-fade-3D-balls.png

Structure – rocksalt (MN)

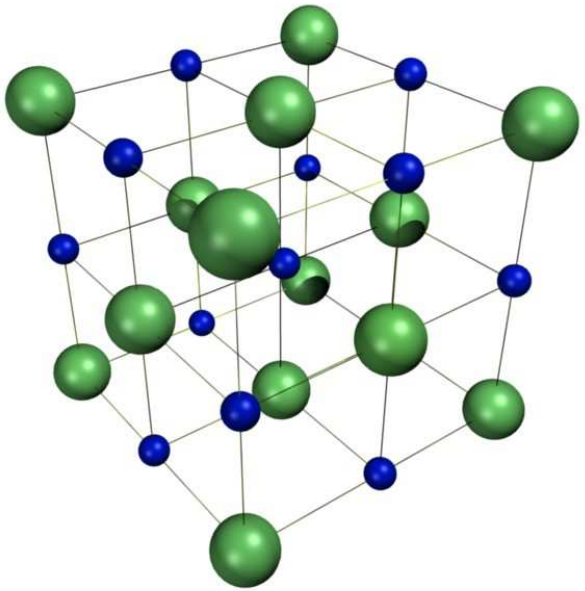

Lattice Vectors

$\mathbf{A}_1 = \frac{1}{2}\,a\,\mathbf{Y} + \frac{1}{2}\,a\,\mathbf{Z}$

$\mathbf{A}_2 = \frac{1}{2}\,a\,\mathbf{X} + \frac{1}{2}\,a\,\mathbf{Z}$

$\mathbf{A}_3 = \frac{1}{2}\,a\,\mathbf{X} + \frac{1}{2}\,a\,\mathbf{Y}$

Basis Vectors

$\mathbf{B}_1 = 0$

$\mathbf{B}_2 = \frac{1}{2}\,\mathbf{A}_1 + \frac{1}{2}\,\mathbf{A}_2 + \frac{1}{2}\,\mathbf{A}_3 = \frac{1}{2}\,a\,\mathbf{X} + \frac{1}{2}\,a\,\mathbf{Y} + \frac{1}{2}\,a\,\mathbf{Z}$

http://commons.wikimedia.org/wiki/File:Nacl-structure.jpg

Structure – cesium chloride (MN)

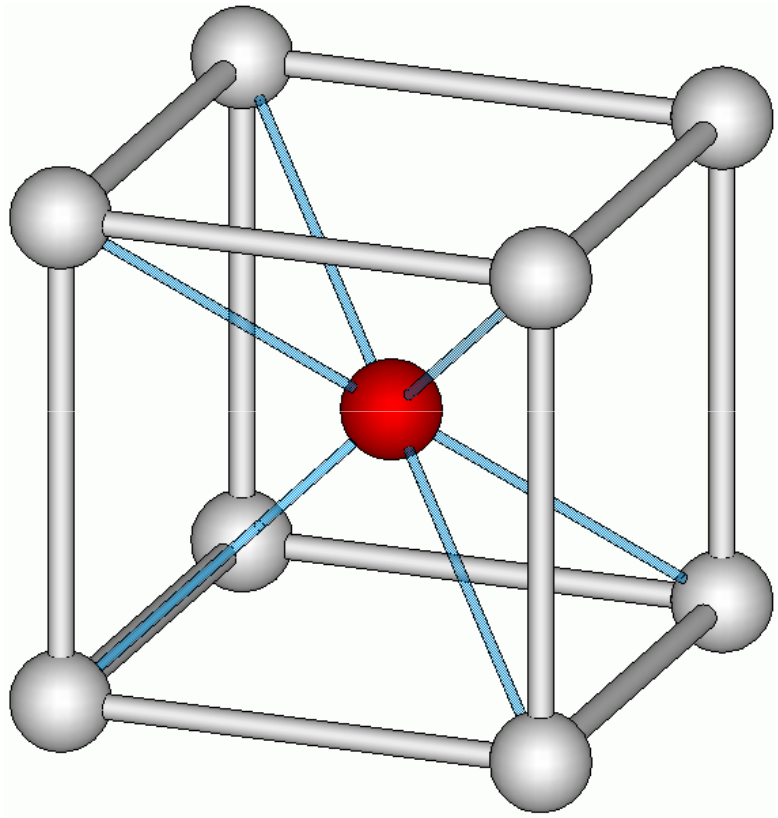

Lattice Vectors

$\mathbf{A}_1 = a\,\mathbf{X}$

$\mathbf{A}_2 = a\,\mathbf{Y}$

$\mathbf{A}_3 = a\,\mathbf{Z}$

Basis Vectors

$\mathbf{B}_1 = 0$

$\mathbf{B}_2 = \frac{1}{2}\mathbf{A}_1 + \frac{1}{2}\mathbf{A}_2 + \frac{1}{2}\mathbf{A}_3 = \frac{1}{2}a\,\mathbf{X} + \frac{1}{2}a\,\mathbf{Y} + \frac{1}{2}a\,\mathbf{Z}$

http://meatfighter.com/puls/

Structure – NbO (MN)

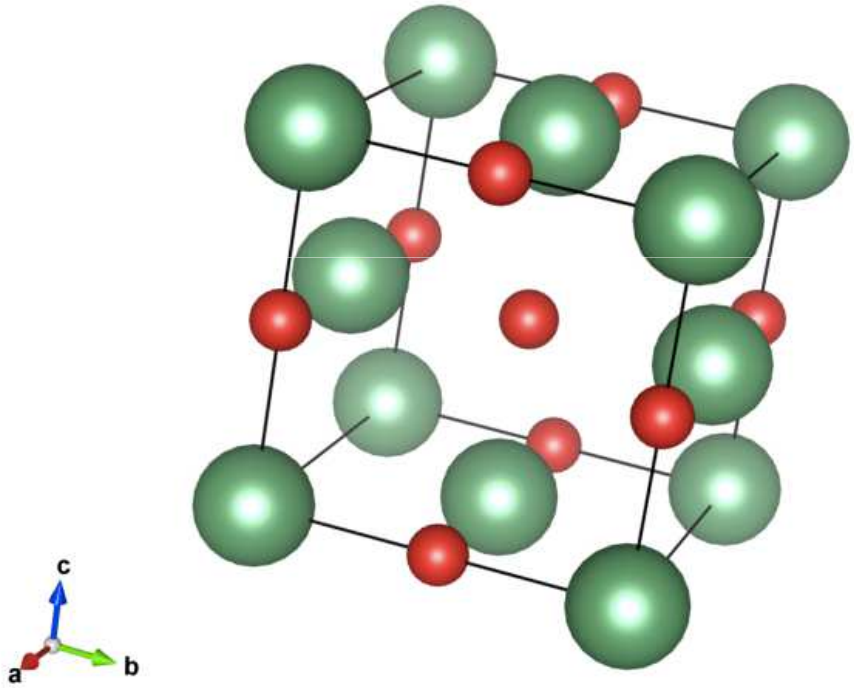

Lattice Vectors

$\mathbf{A}_1 = a\,\mathbf{X}$

$\mathbf{A}_2 = a\,\mathbf{Y}$

$\mathbf{A}_3 = a\,\mathbf{Z}$

Basis Vectors

$\mathbf{B}_1 = 0$

$\mathbf{B}_2 = \frac{1}{2}\mathbf{A}_1 + \frac{1}{2}\mathbf{A}_2$

$\mathbf{B}_3 = \frac{1}{2}\mathbf{A}_1 + \frac{1}{2}\mathbf{A}_3$

$\mathbf{B}_4 = \frac{1}{2}\mathbf{A}_2$

$\mathbf{B}_5 = \frac{1}{2}\mathbf{A}_3$

$\mathbf{B}_6 = \frac{1}{2}\mathbf{A}_1 + \frac{1}{2}\mathbf{A}_2 + \frac{1}{2}\mathbf{A}_3$

M	a (Å)			C_{11} (GPa)			C_{12} (GPa)			C_{44} (GPa)			Mechanical Stability		
	zb	rs	cc	zb	rs	cc	zb	rs	cc	zb	rs	cc	zb	rs	cc
Sc	4.883	4.503	2.768	179.6	434.7	502.8	132.9	97.7	42.2	71.8	160.9	-119.2	S	S	**U**
		4.516[a]			390[a]			105[a]			166[a]				
		4.48[b]			386.4[b]			101[b]			171.7[b]				
		4.44[c]													
Ti	4.569	4.221	2.607	307.2	657.7	619.6	165.2	121.0	106.2	99.2	165.4	39.6	S	S	S
		4.253[a]			560[a]			135[a]			163[a]				
		4.218[b]			591.8[b]			123.4[b]			184.7[b]				
		4.241[c]			625[d]			165[d]			163[d]				
					507[e]			96[e]			163[e]				
V	4.407	4.095	2.521	328.1	685.8	969.5	213.0	172.8	33.6	42.8	121.5	160.3	S	S	S
		4.127[a]			660[a]			174[a]			118[a]				
		4.088[b]			695.9[b]			146.7[b]			152.8[b]				
		4.139[c]			533[d]			135[d]			133[d]				
Cr	4.302	4.025	2.477	341.1	636.0	894.3	240.2	218.1	102.1	-66.2	7.0	17.0	**U**	S	S
		4.048[b]			510.5[b]			217.2[b]			6.8[b]				
Mn	4.229	3.985	2.459	352.0	616.0	898.6	257.6	229.7	98.2	33.5	-10.9	38.3	S	**U**	S
Fe	4.201	3.968	2.459	356.9	485.9	825.9	258.7	281.4	110.0	112.4	-37.2	29.4	S	**U**	S
Co	4.221	3.971	2.485	322.5	468.0	542.2	242.9	258.1	191.8	68.2	65.7	17.8	S	S	S
Ni	4.289	4.029	2.520	255.5	434.1	529.5	223.5	212.4	151.0	46.7	87.7	-5.5	S	S	**U**
Cu	4.398	4.136	2.585	202.7	352.3	356.0	180.0	171.0	160.8	39.4	62.6	7.5	S	S	S
Zn	4.530	4.258	2.674	161.3	288.7	231.5	143.0	139.2	150.7	45.0	67.3	-39.0	S	S	**U**

a GGA, D. Holec *et al.*, Phys. Rev. B **85,** 064101 (2012).
b Avg. of LDA & GGA, M. G. Brik *et al.*, Comput. Mater. Sci. **51**, 380 (2012).
c Exp., Powder diffraction files: ScN 00-045-0978, TiN 03-065-0565, VN 00-035-0768.
d Exp., J. O. Kim *et al.*, J. Appl. Phys. **72**, 1805 (1992).
e Exp., W. J. Meng *et al.*, Thin Solid Films **271**, 108 (1995).

Comparison of direct *ab initio* results with experimental values

M	a (Å)			C_{11} (GPa)			C_{12} (GPa)			C_{44} (GPa)		
	zb	rs	cc	zb	rs	cc	zb	rs	cc	zb	rs	cc
Sc	4.883	4.503	2.768	179.6	434.7	502.8	132.9	97.7	42.2	71.8	160.9	-119.2
		4.44[a]										
Ti	4.569	4.221	2.607	307.2	657.7	619.6	165.2	121.0	106.2	99.2	165.4	39.6
		4.241[a]			625[b]			165[b]			163[b]	
					507[c]			96[c]			163[c]	
V	4.407	4.095	2.521	328.1	685.8	969.5	213.0	172.8	33.6	42.8	121.5	160.3
		4.139[a]			533[b]			135[b]			133[b]	

a Powder diffraction files: ScN 00-045-0978, TiN 03-065-0565, VN 00-035-0768.
b J. O. Kim *et al.*, J. Appl. Phys. **72**, 1805 (1992).
c W. J. Meng *et al.*, Thin Solid Films **271**, 108 (1995).

Polycrystalline properties

B (bulk modulus), *G* (shear modulus) and *E* (Young's modulus)

M	B (GPa)			G (GPa)			E (GPa)		
	zb	rs	cc	zb	rs	cc	zb	rs	cc
Sc	148.5	210.0	195.7	45.8	163.9	**U**	124.7	390.2	**U**
Ti	212.6	299.9	277.3	86.8	200.9	93.2	229.1	492.8	251.4
V	251.4	343.8	345.6	48.2	164.7	250.5	135.9	426.1	605.2
Cr	273.9	357.4	366.2	**U**	49.6	98.1	**U**	142.1	270.3
Mn	289.1	358.5	365.0	38.4	**U**	121.5	110.4	**U**	328.1
Fe	291.4	349.5	348.6	80.6	**U**	103.6	221.5	**U**	282.8
Co	269.5	328.0	308.6	55.0	79.3	54.2	154.4	220.2	153.7
Ni	234.2	286.3	277.1	30.4	96.3	**U**	87.5	259.8	**U**
Cu	187.6	231.5	225.9	24.0	72.6	27.7	69.1	197.3	79.8
Zn	149.1	189.1	177.6	24.1	70.2	**U**	68.6	187.3	**U**

zb (zincblende)
rs (rocksalt)
cc (cesium chloride)

Polycrystalline properties

P_C (Cauchy's pressure), v (Poisson's ratio) and k (Pugh's ratio)

M	P_C (GPa)			v			k		
	zb	rs	cc	zb	rs	cc	zb	rs	cc
Sc	61.1	-63.3	U	0.36	0.19	U	0.31	0.78	U
Ti	66.0	-44.4	66.6	0.32	0.23	0.35	0.41	0.67	0.34
V	170.2	51.3	-126.7	0.41	0.29	0.21	0.19	0.48	0.72
Cr	U	211.1	85.1	U	0.43	0.38	U	0.14	0.27
Mn	224.1	U	59.9	0.44	U	0.35	0.13	U	0.33
Fe	146.3	U	80.6	0.37	U	0.36	0.28	U	0.30
Co	174.7	192.4	174.1	0.40	0.39	0.42	0.20	0.24	0.18
Ni	176.8	124.7	U	0.44	0.35	U	0.13	0.34	U
Cu	140.6	108.4	153.3	0.44	0.36	0.44	0.13	0.31	0.12
Zn	98.1	72.0	U	0.42	0.33	U	0.16	0.37	U

zb (zincblende)
rs (rocksalt)
cc (cesium chloride)

Polycrystalline properties

H_V (Vicker's hardness) and θ_D (Debye temperature)

M	H_V (GPa)			θ_D (K)		
	zb	rs	cc	zb	rs	cc
Sc	3.6	25.7	**U**	506.8	901.5	**U**
Ti	7.8	24.9	6.6	654.9	947.1	648.4
V	2.2	14.8	31.9	473.6	830.9	1002.8
Cr	**U**	1.5	5.3	**U**	457.0	630.4
Mn	1.2	**U**	7.9	403.5	**U**	681.4
Fe	4.8	**U**	6.2	573.8	**U**	626.2
Co	2.6	4.1	2.2	466.8	542.6	448.9
Ni	1.0	6.8	**U**	352.1	600.1	**U**
Cu	0.8	5.1	0.9	306.8	511.9	318.3
Zn	1.1	6.0	**U**	307.6	502.9	**U**

zb (zincblende)
rs (rocksalt)
cc (cesium chloride)

V (unit cell volume) and *B* (bulk modulus)

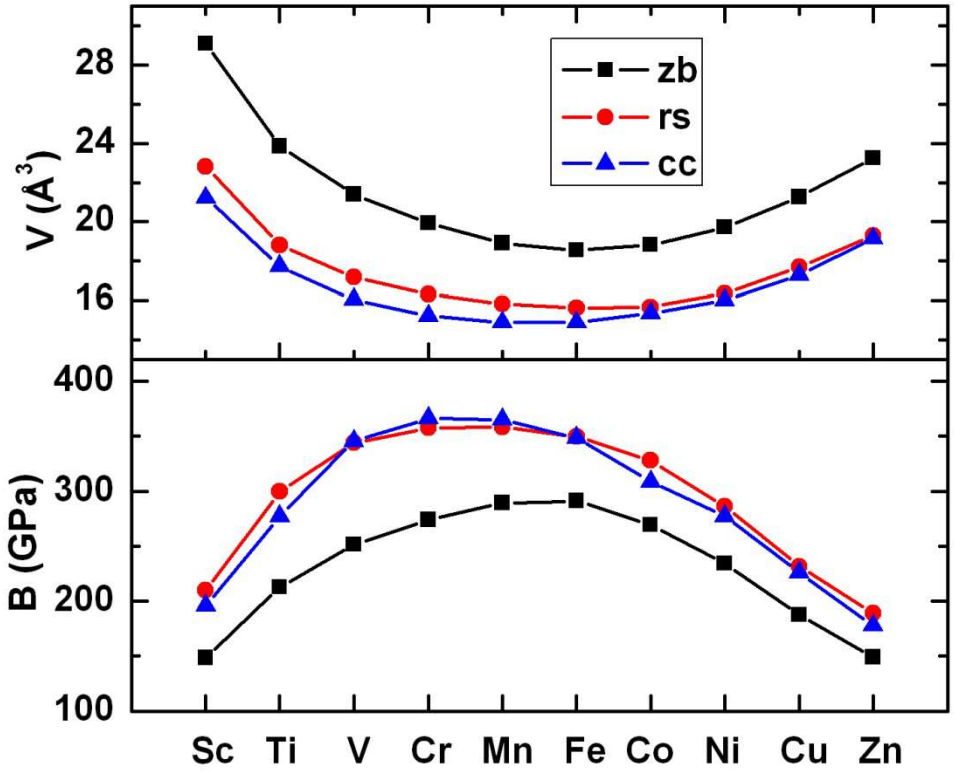

$$B = (C_{11} + 2C_{12})/3$$

P_C, ν and k

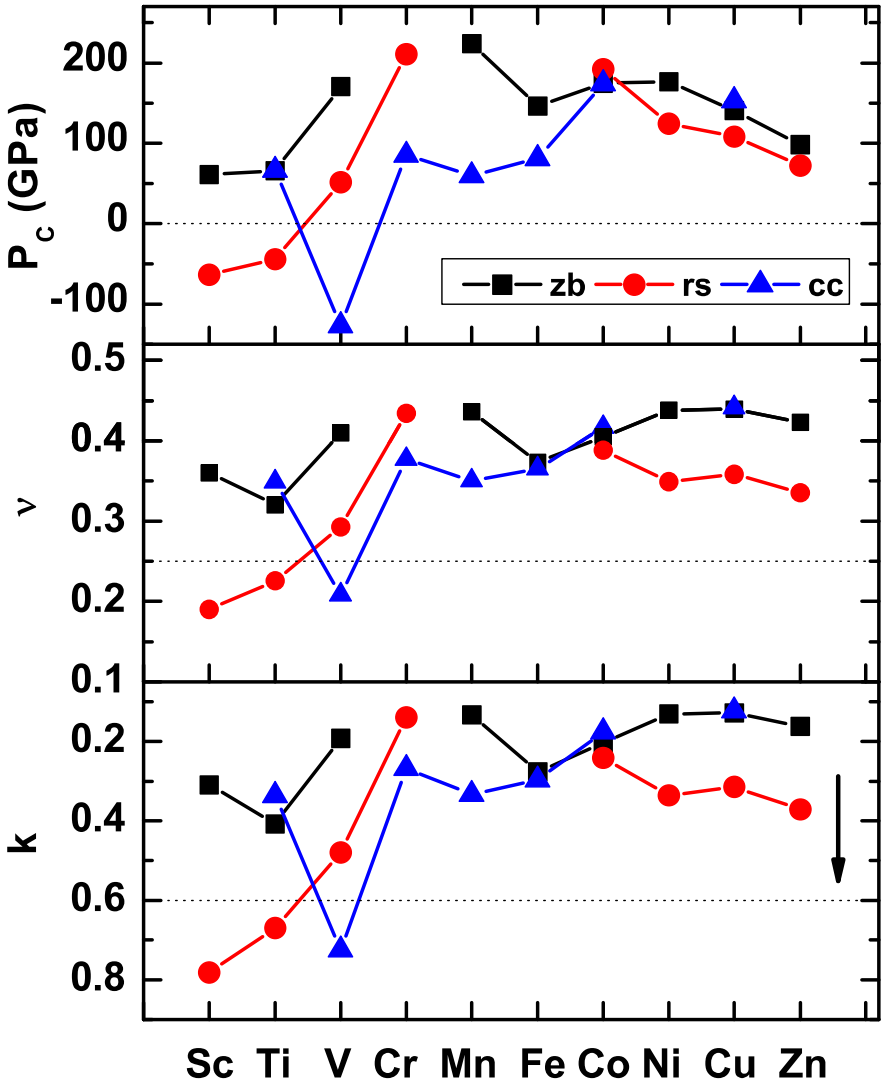

P_c (Cauchy's pressure)

$P_C = C_{12} - C_{44}$

ν (Poisson's ratio)

$\nu = (3B - 2G)/[2(3B + G)]$

k (Pugh's ratio)

$k = G/B$

Chen's formulation for calculating H_V (Vicker's Hardness)

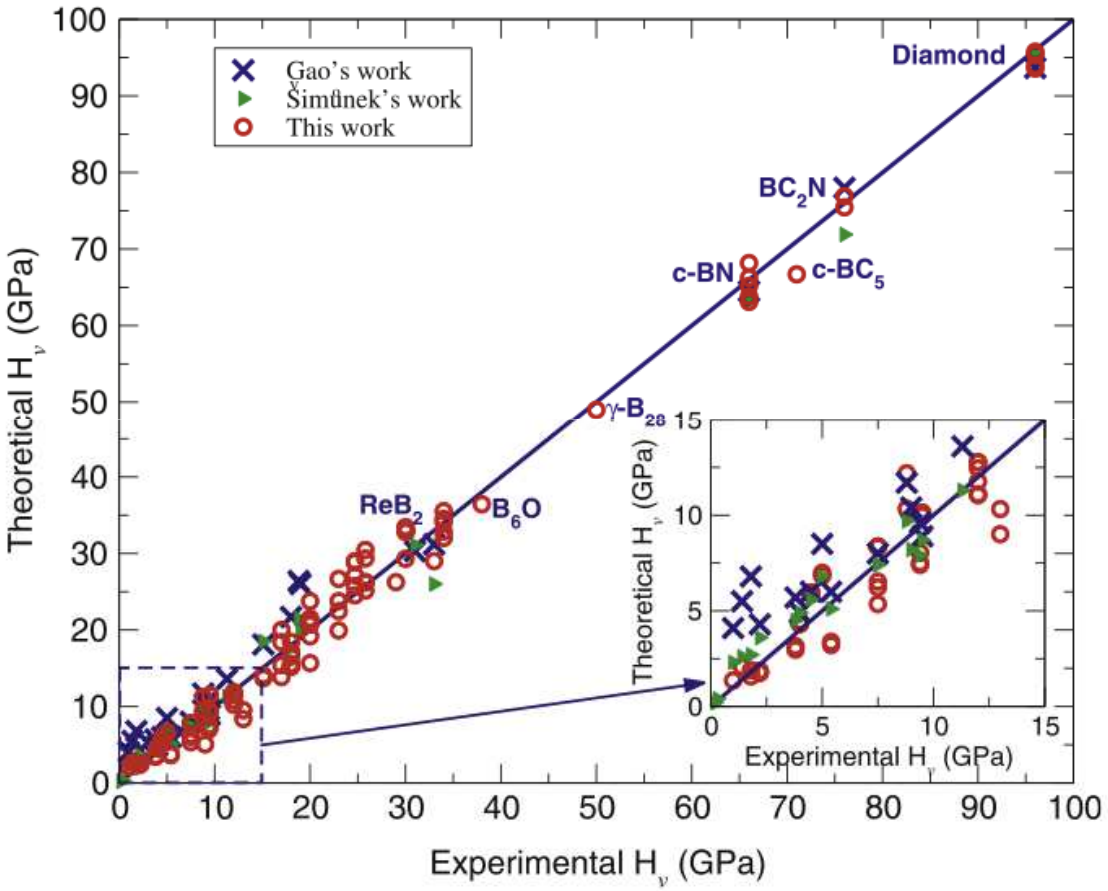

$$B = (C_{11} + 2C_{12})/3$$

$$G_v = [(C_{11} - C_{12}) + 3C_{44}]/5$$

$$G_R = [5(C_{11} - C_{12})C_{44}]/(4C_{44} + 3C_{11} - 3C_{12})$$

$$G = G_{VRH} = (G_v + G_R)/2$$

$$k = G/B$$

$$H_v = 2\left(k^2 G\right)^{0.585} - 3$$

X. Q. Chen *et al.*, Intermetallics **19**, 1275 (2011)

Tian's alternative for calculating H_V (Vicker's Hardness)

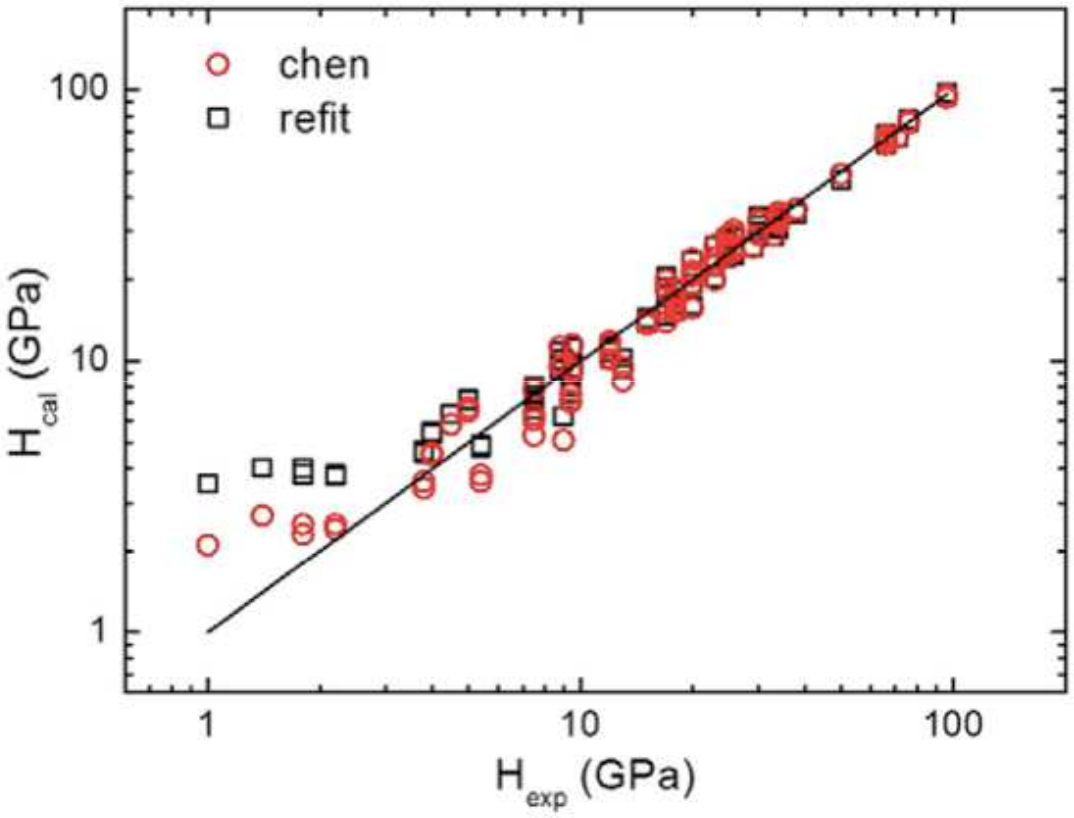

$$B = (C_{11} + 2C_{12})/3$$

$$G_v = [(C_{11} - C_{12}) + 3C_{44}]/5$$
$$G_R = [5(C_{11} - C_{12})C_{44}]/(4C_{44} + 3C_{11} - 3C_{12})$$
$$G = G_{VRH} = (G_v + G_R)/2$$

$$k = G/B$$

$$H_V = 0.92k^{1.137}G^{0.708}$$

Y. Tian *et al.*, Int. J. Refract. Met. Hard Mater. **33**, 93 (2012).

Crystal	H_{Exp} (GPa)	H_{Tian} (GPa)	$H_{Simunek}$ (GPa)	H_{Xue} (GPa)	H_{Chen} (GPa)
C	96[a]	93.6	95.4[b]	90[e]	94.6[f]
Si	12[a]	13.6	11.3[b]	14[e]	11.2[f]
Ge	8.8[b]	11.7	9.7[b]	11.4[e]	10.4[f]
SiC	31[b]	30.3	31.1[b]	27.8[e]	33.8[f]
BN	63[a]	64.5	63.2[b]	47.7[e]	65.3[f]
BP	33[a]	31.2	26[b]	24.9[e]	29.3[f]
BAs	19[b]	26	19.9[b]	21.1[e]	–
AlN	18[a]	21.7	17.6[b]	14.5[e]	16.8[f]
AlP	9.4[a]	9.6	7.9[b]	7.4[e]	7.2[f]
AlAs	5.0[a]	8.5	6.8[b]	6.3[e]	6.6[f]
AlSb	4.0[a]	4	4.9[b]	4.9[e]	4.4[f]
GaN	15.1[a]	18.1	18.5[b]	13.5[e]	13.9[f]
GaP	9.5[a]	8.9	8.7[b]	8[e]	9.9[f]
GaAs	7.5[a]	8	7.4[b]	7.1[e]	7.8[f]
GaSb	4.5[a]	6	5.6[b]	4.5[e]	5.8[f]
InN	9[a]	10.4	8.2[b]	7.4[e]	7.4[f]
InP	5.4[a]	6	5.1[b]	3.9[e]	3.7[f]
InAs	3.8[a]	3.8	5.7[b]	4.5[e]	3.3[f]
InSb	2.2[a]	4.3	3.6[b]	2.2[e]	2.4[f]
ZnS	1.8[b]	6.8	2.7[b]	2.4[e]	2.4[f]
ZnSe	1.4[b]	5.5	2.6[b]	1.8[e]	2.7[f]
ZnTe	1[b]	4.1	2.3[b]	0.9[e]	2.1[f]
TiC	32[c]	34	18.8[b]	23.9[e]	27[f]
TiN	20.6[c]	21.6	18.7[b]	23.8[h]	23.3[f]
ZrC	25[c]	21	10.7[g]	15.7[h]	27.5[f]

Y. Tian *et al.*, Int. J. Refract. Met. Hard Mater. **33**, 93 (2012).

Crystal	H_{Exp} (GPa)	H_{Tian} (GPa)	$H_{Simunek}$ (GPa)	H_{Xue} (GPa)	H_{Chen} (GPa)
ZrN	15.8[c]	16.7	10.8[g]	15.9[h]	–
HfC	26.1[c]	26.8	10.9[g]	15.6[h]	–
HfN	16.3[c]	18	10.6[g]	15.2[h]	19.2[f]
VC	27.2[c]	23	25.2[g]	17.5[h]	26.2[f]
VN	15.2[c]	14.9	26.5[g]	16.5[h]	–
NbC	17.6[c]	16.1	18.3[b]	12.8[h]	15.4[f]
NbN	13.7[c]	13.6	19.5[b]	12[h]	14.7[f]
TaC	24.5[c]	26	19.9[g]	14.7[h]	–
TaN	22[c]	20	21.2[g]	14.3[h]	–
CrN	11[c]	11	36.6[g]	19.2[h]	–
WC	30[c]	31	21.5[b]	20.6[e]	31.3[f]
Re_2C	17.5[j]	19.7[j]	11.5[g]	16.2[h]	26.4[i]
Al_2O_3	20[c]	18.8	13.5[g]	18.4[h]	20.3[i]
MgO	3.9[d]	4.5	4.4[g]	5.4[h]	24.8[i]
LiF	1[d]	0.8	2.2[g]	–	8.5[i]
NaF	0.6[d]	0.85	1[g]	–	5.7[i]
NaCl	0.2[d]	0.4	0.4[b]	–	2.4[i]
KCl	0.13[d]	0.18	0.2[b]	–	2.3[i]
KBr	0.1[d]	0.23	0.2[g]	–	0.1[i]

[a] Reference [34].
[b] Reference [37].
[c] Reference [32].
[d] Reference [60].
[e] Reference [58].
[f] Reference [30].
[g] Calculated by authors using method [36].
[h] Caculated using [35].
[i] Calculated with [30].
[j] Referenece [52].

G (shear modulus) and H_{VA} (Tian's)

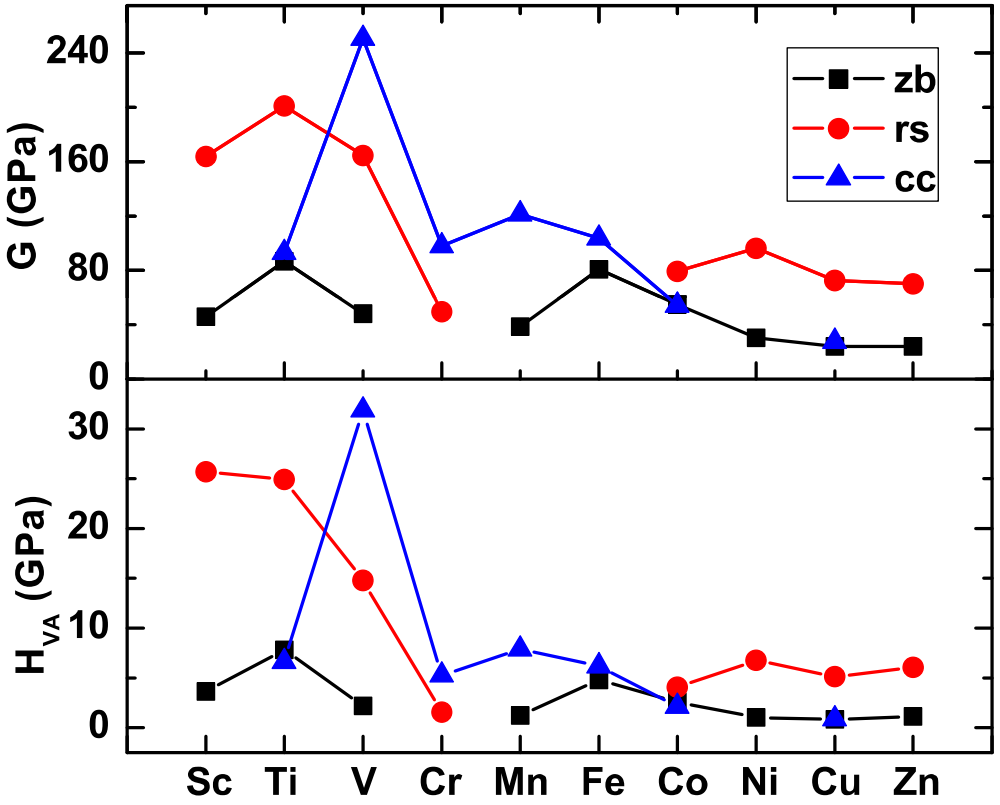

$G_v = [(C_{11} - C_{12}) + 3C_{44}]/5$

$G_R = [5(C_{11} - C_{12})C_{44}]/$
$(4C_{44} + 3C_{11} - 3C_{12})$

$G = G_{VRH} = (G_v + G_R)/2$

$H_{VA} = 0.92\, k^{1.137}\, G^{0.708}$

ϑ_D (Debye temperature) vs $f(H_{VA})$

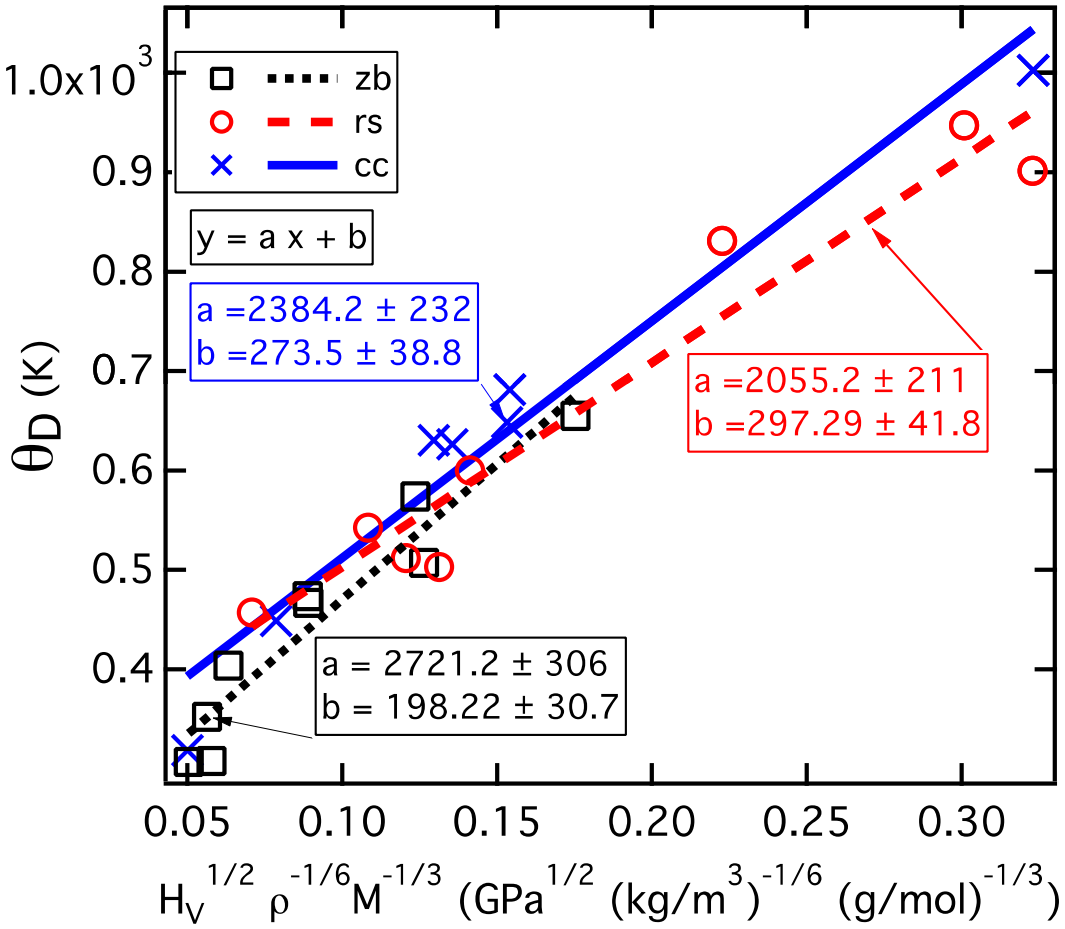

$$\theta_D = \frac{h}{k_B}\left[\frac{3n}{4\pi}\left(\frac{N_A\rho}{M}\right)\right]^{1/3} v_m$$

where $v_m = \left[\frac{1}{3}\left(\frac{2}{v_t^3} + \frac{1}{v_l^3}\right)\right]^{-1/3}$

$v_t = \left(\frac{G}{\rho}\right)^{1/2}$ and $v_l = \left(\frac{3B+4G}{3\rho}\right)^{1/2}$

$H_{VA} = 0.92\ k^{1.137}\ G^{0.708}$

P. Deus *et al.*, Cryst. Res. Technol. **18**, 491 (1983).

Correlation of stability with DOS

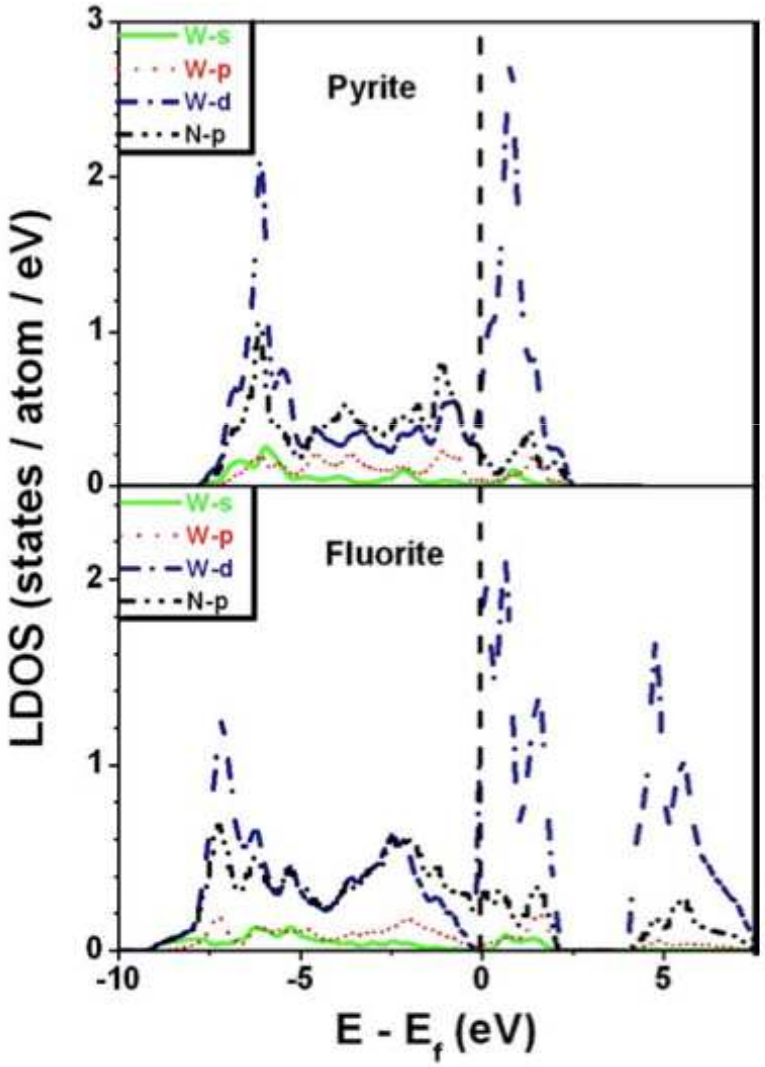

- Pyrite-structured WN_2 is stable, and DOS at E_F is small
- Fluorite-structured WN_2 is unstable, and DOS at E_F is large

S. K. R. Patil *et al.*, Thin Solid Films **517**, 824 (2008)

Correlation of C_{44} (indicating H_V and stability) with TDOS

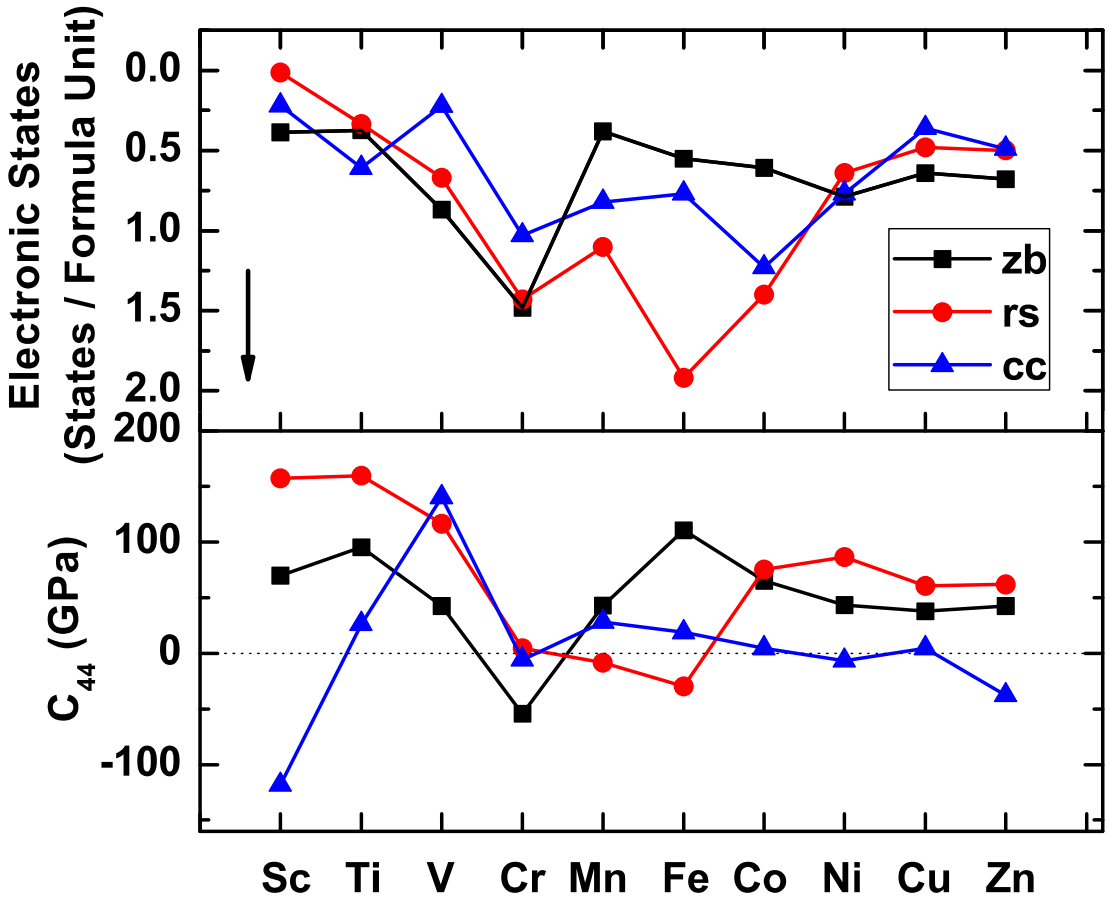

Correlation of C_{44} (indicating H_V and stability) with TDOS of NbO-type

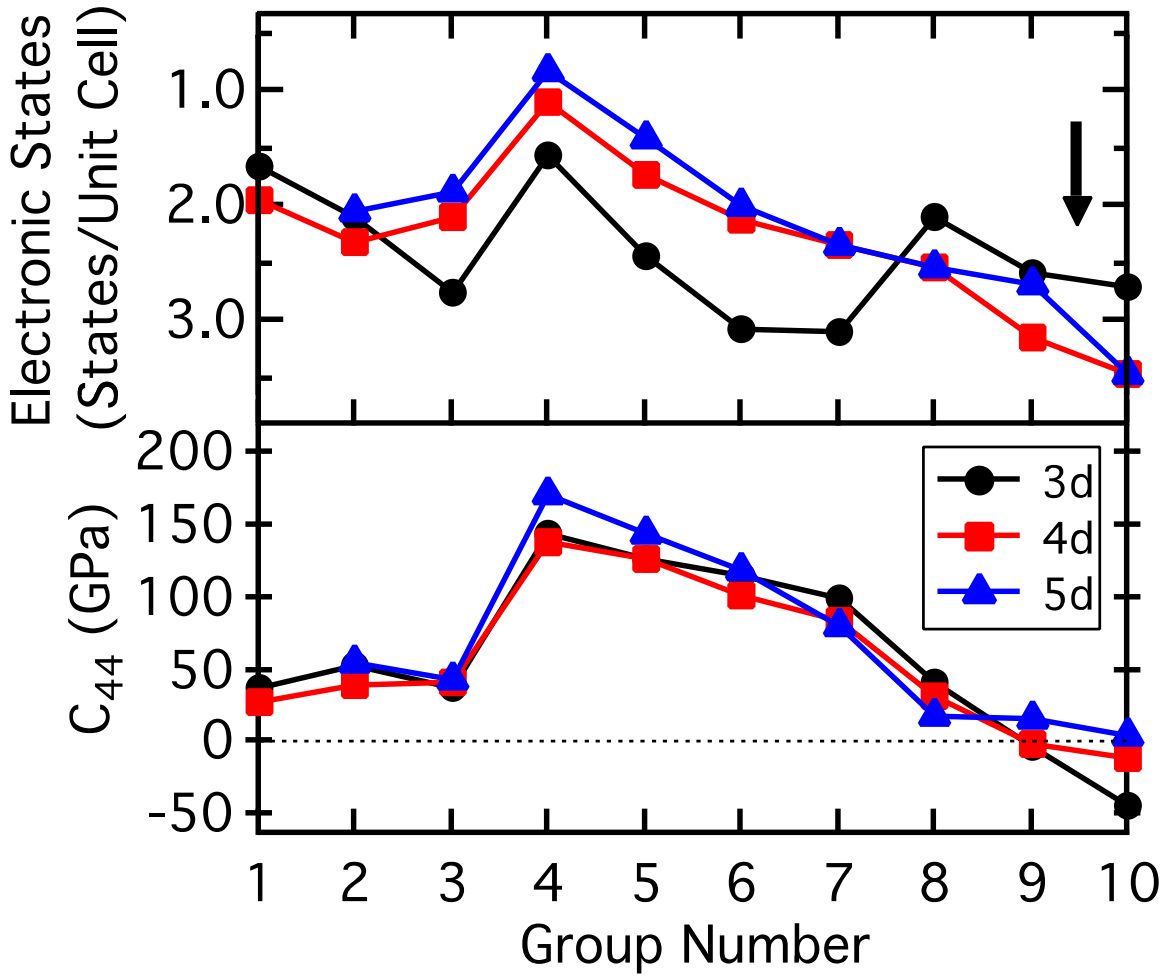

LDOS - zincblende

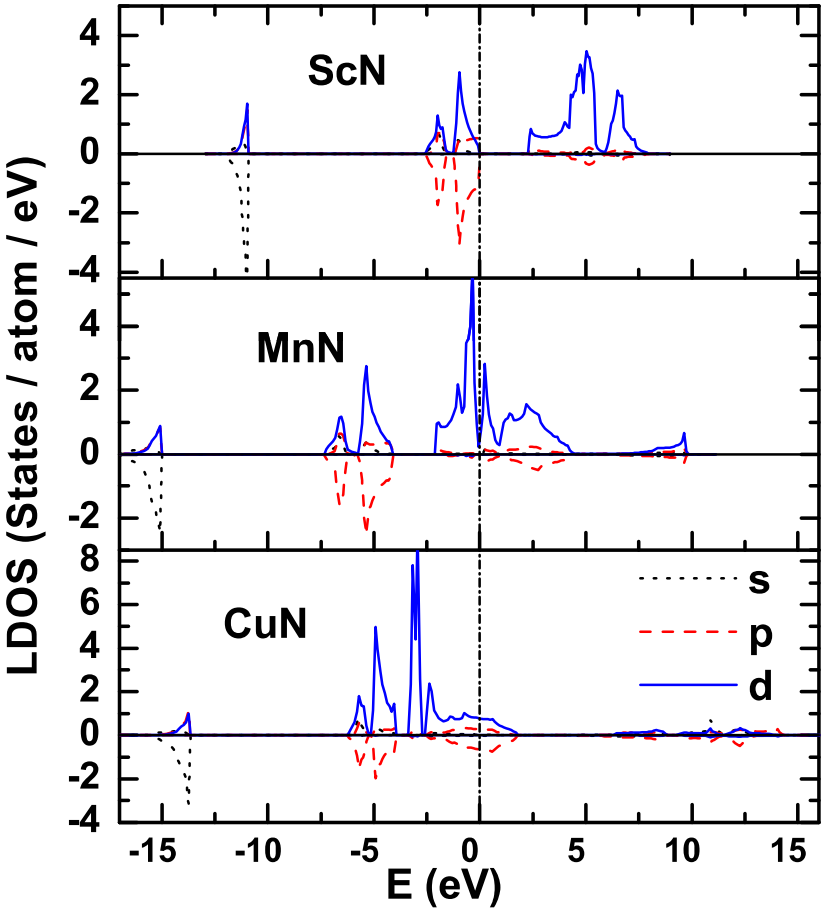

As transition metal goes from left to right in the 3d row, more states shift below E_F, peaks becoming sharper.

LDOS - rocksalt

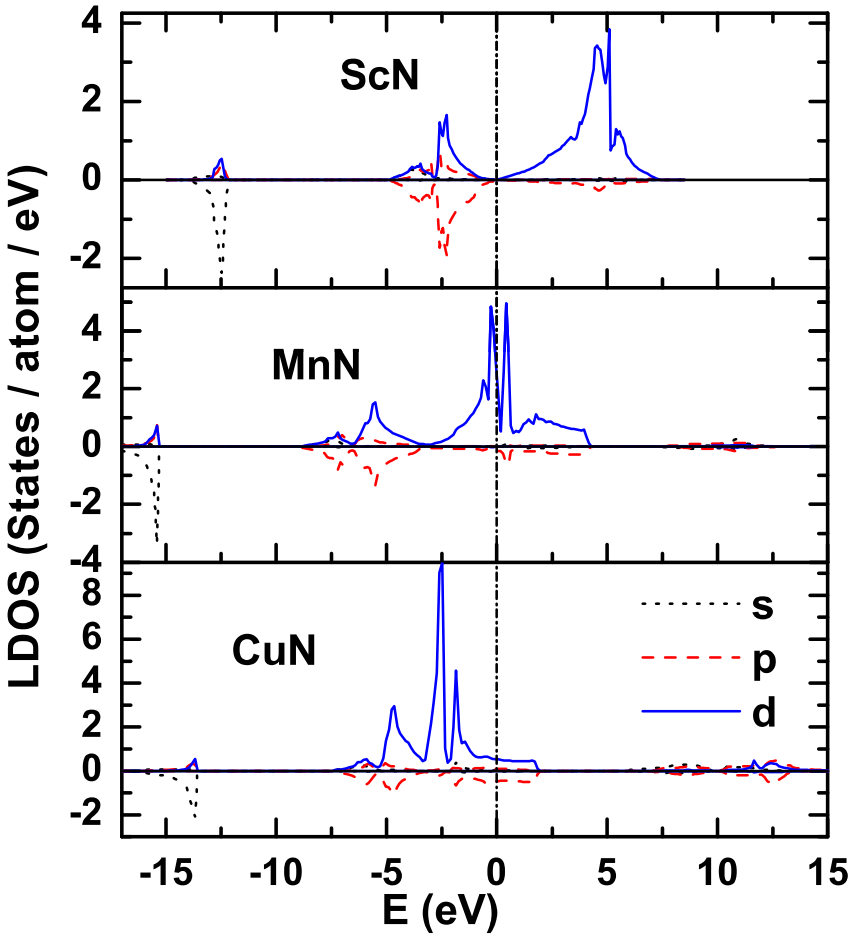

As transition metal goes from left to right in the 3d row, more states shift below E_F, peaks becoming sharper.

LDOS – cesium chloride

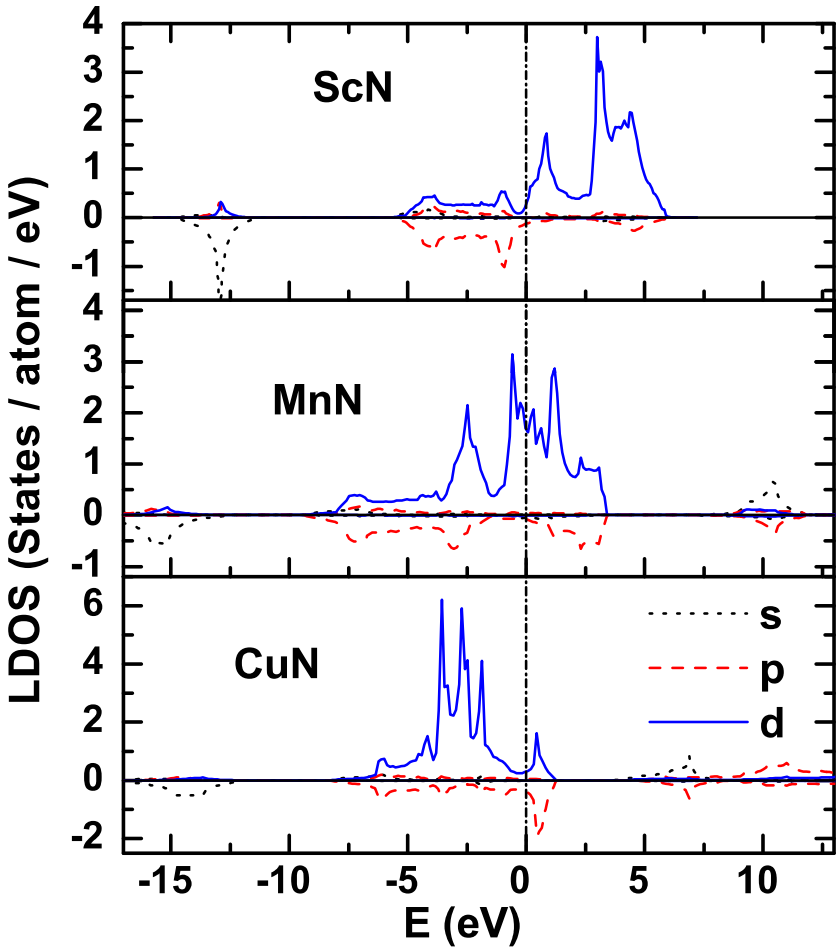

As transition metal goes from left to right in the 3d row, more states shift below E_F, peaks becoming sharper.

Bader analysis of NbO-type

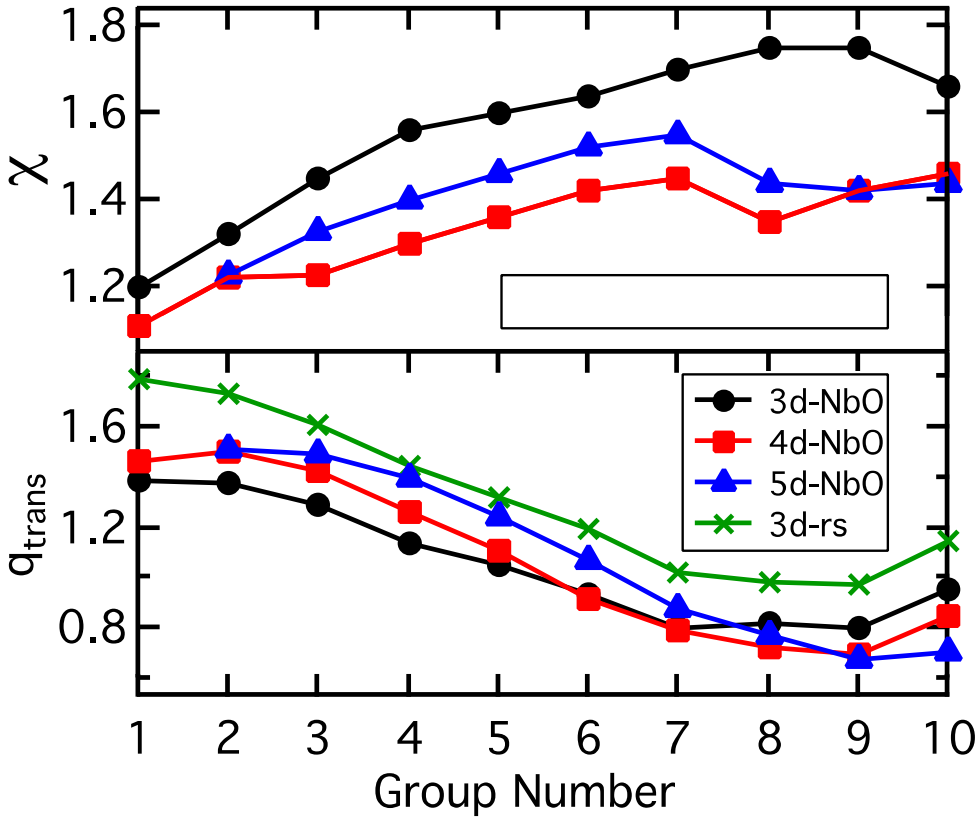

χ (nitrogen): 3.07

χ (electronegativity) from
A. L. Allred *et al.*, J. Inorg. Nucl. Chem. **5**, 264 (1958).

q_{trans} (charge transfer from transition metal to nitrogen using Bader's scheme)

Bader analysis program from
W. Tang *et al.*, J. Phys.: Condens. Matter 21, 084204 (2009)
E. Sanville *et al.*, J. Comp. Chem. 28, 899-908 (2007)
G. Henkelman *et al.*, Comput. Mater. Sci. 36, 254-360 (2006)

H_{VA} vs P_C (Cauchy's pressure)

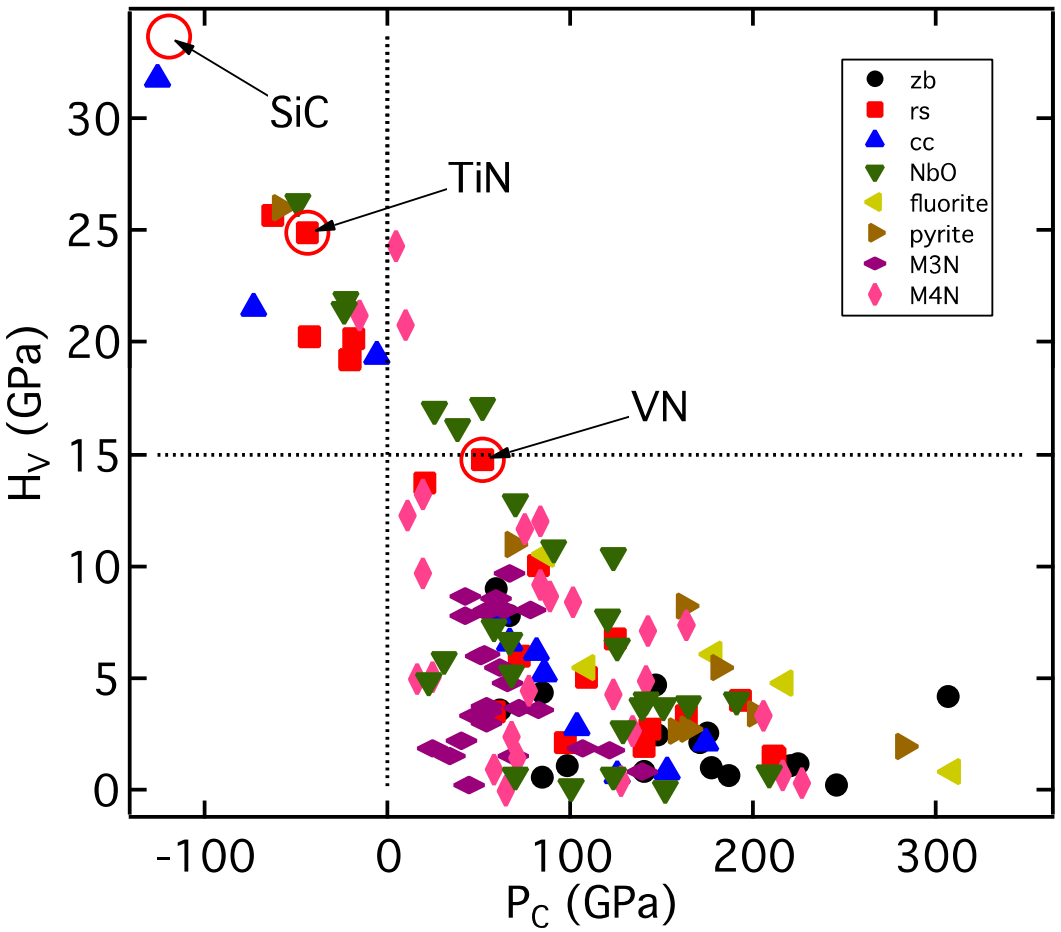

Data partly from

W. Chen *et al.*, J. Alloys Compd. **499**, 243 (2010).
E. J. Zhao *et al.*, Comput. Mater. Sci. **47**, 1064 (2010).
E. J. Zhao *et al.*, J. Solid State Chem. **181**, 2814 (2008).

H_{VA} vs k (Pugh's ratio) x-axis inverted

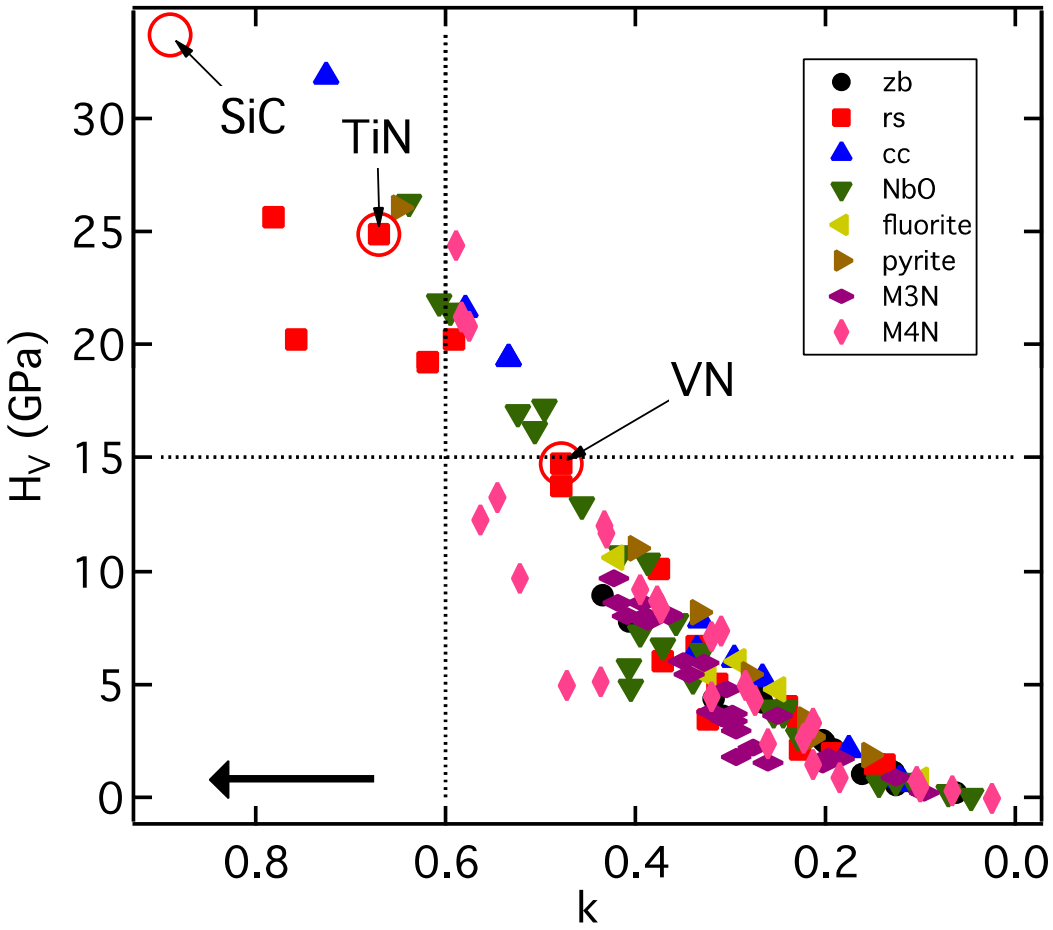

H_{VA} vs ν (Poisson's ratio)

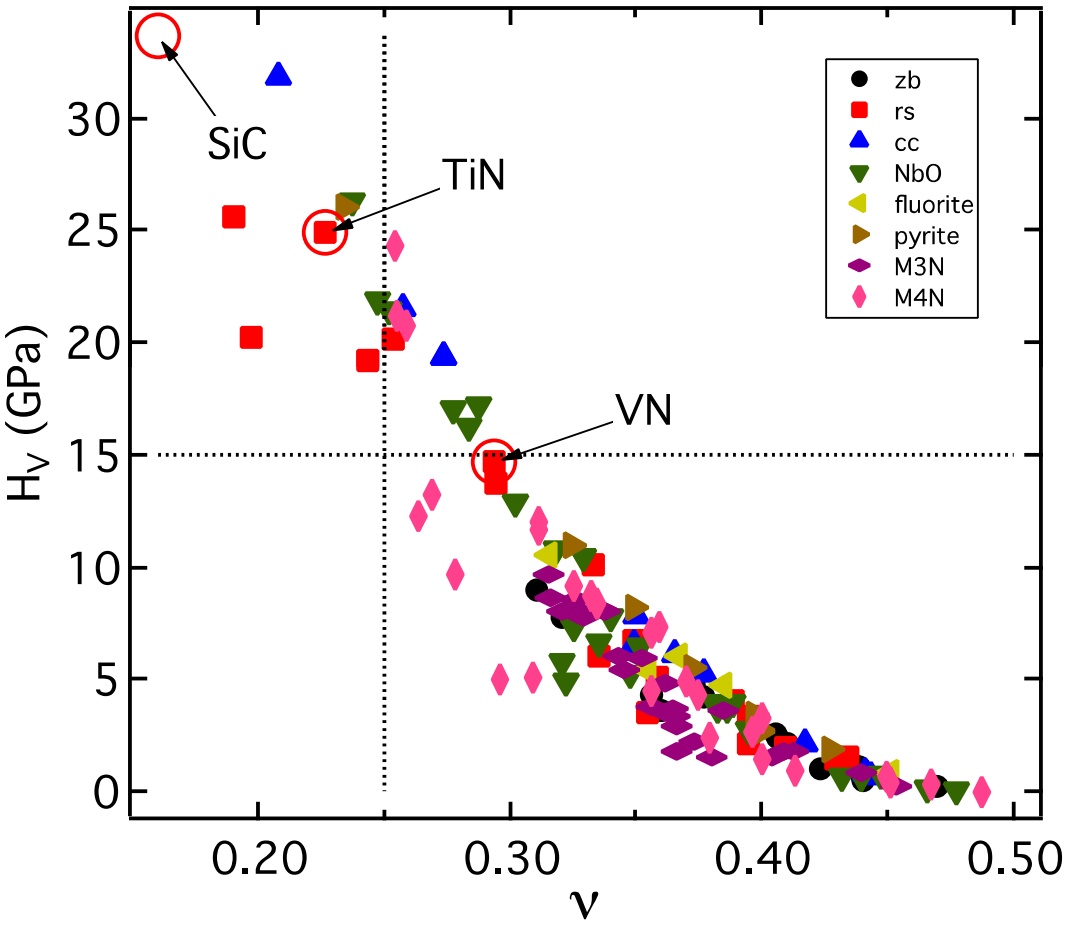

k vs P_C

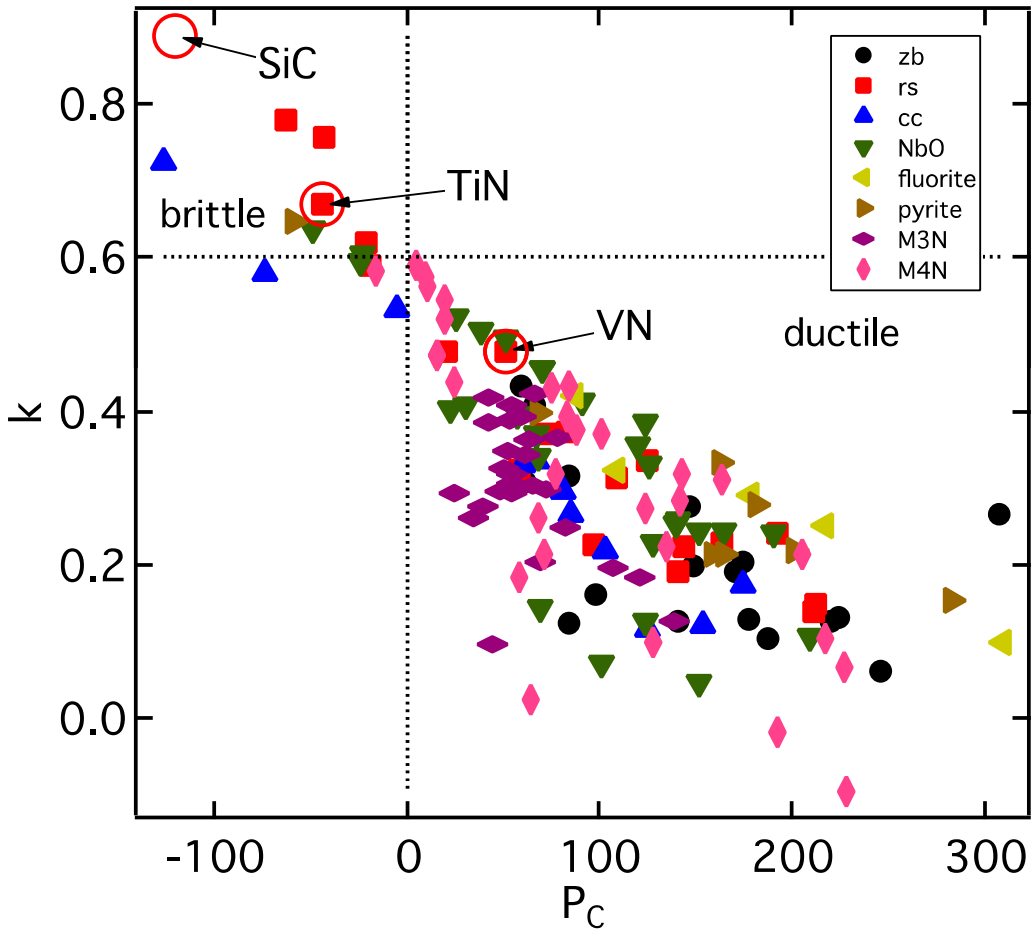
SiC
TiN
VN
brittle
ductile
zb
rs
cc
NbO
fluorite
pyrite
M3N
M4N
0.8
0.6
0.4
0.2
0.0
κ
-100
0
100
200
300
P_C

Nitrides with $H_{VA} \geq 15$ GPa

Material	a (A)	C_{11}	C_{12}	C_{44}	B (GPa)	G (GPa)	ν	k	P_C (GPa)	H_{VA} (GPa)
diamond	3.548	1079.8	131.4	577.2	447.5	533.5	0.07	1.19	-445.80	95.80
SiC	4.345	396.5	128.5	249.2	217.8	194.3	0.16	0.89	-120.70	33.70
M_4N-Mn_4N	3.653	769.2	127.6	143.8	341.4	199.5	0.26	0.58	-16.20	21.23
M_4N-Tc_4N	3.971	670.3	184.1	174.3	346.1	199.2	0.26	0.58	9.81	20.83
M_4N-Re_4N	3.993	772.4	221.1	217.0	404.8	238.8	0.25	0.59	4.06	24.37
rs-ScN	4.503	434.7	97.7	160.9	210.0	163.9	0.19	0.78	-63.27	25.67
rs-TiN	4.221	657.7	121.0	165.4	299.9	200.9	0.23	0.67	-44.40	24.93
rs-VN	4.095	685.8	172.8	121.5	343.8	164.7	0.29	0.48	51.32	14.78
rs-YN	4.890	319.0	84.0	127.0	162.3	123.1	0.20	0.76	-43.00	20.28
rs-ZrN	4.580	563.0	101.0	122.0	255.0	158.0	0.24	0.62	-21.00	19.23
rs-HfN	4.436	704.9	111.8	131.0	309.5	182.9	0.25	0.59	-19.20	20.22
cc-VN	2.521	969.5	33.6	160.3	345.6	250.5	0.21	0.72	-126.72	31.85
cc-TaN	2.731	1006.0	33.0	107.0	357.3	207.2	0.26	0.58	-74.00	21.60
cc-ReN	2.679	900.0	122.0	128.0	381.3	203.7	0.27	0.53	-6.00	19.45
NbO-CrN	3.802	724.9	123.2	146.9	323.8	196.6	0.25	0.61	-23.72	21.94
NbO-MnN	3.744	683.9	156.9	131.4	332.6	174.3	0.28	0.52	25.55	17.04
NbO-MoN	4.096	763.6	115.3	139.6	331.4	197.1	0.25	0.59	-24.28	21.47
NbO-TcN	4.030	686.0	169.6	131.6	341.7	173.0	0.28	0.51	37.94	16.30
NbO-WN	4.092	857.9	123.1	172.5	368.1	234.7	0.24	0.64	-49.36	26.30
NbO-ReN	4.041	761.0	200.9	149.5	387.6	192.7	0.29	0.50	51.37	17.24
pyrite-PtN_2	4.792	845.0	101.0	160.0	349.0	226.0	0.23	0.65	-59.00	26.06

Database

Cubic forms of 3d, 4d and 5d transition metal nitrides in M:N ratios from 4:1 to 1:1 to 1:3. Dark green regions have completed *ab initio* results!

Structures	Formula	Stoichiometry	3d	4d	5d
M_4N	M_4N	4:1			
Anti-ReO3	M_3N	3:1			
Zincblende	MN	1:1			
Rocksalt	MN	1:1			
Cesium chloride	MN	1:1			
NbO	MN	1:1			
Spinel	M_3N_4	0.75:1			
Fluorite	MN_2	0.5:1			
Pyrite	MN_2	0.5:1			
Skutterudite	MN_3	0.33:1			

Summary

- Computed single crystal *V*, C_{11}, C_{12}, C_{44}, LDOS and band structures
- Multi-crystal average of *B*, *G*, *E*, ν, *k*, H_V, ϑ_D, T_m.
- Showed correlations of hardness and ductility
- Importance of spread out bands and bonding between M-p orbitals and N-d orbitals
- Inverse correlation of DOS at E_F and C_{44} or stability

Future

- Create Web database of 10 cubic binary nitride phases
- Some search ability will exist
- Hexagonal structures
- Ternaries

Hexagonal structures

- Apart from the cubic phases, there are also **experimental** studies of hexagonal structures.
  - AlN, I. W. Kim *et al.*, Appl. Phys. Lett. **78**, 892, (2001)
  - IrN_2, A. F. Young *et al.*, Phys. Rev. Lett. **96**, 155501, (2006)
  - ReN_2, F. Kawamura *et al.*, Appl. Phys. Lett. **100**, 251910, (2012)
  - Re_3N, A. Friedrich *et al.*, Phys. Rev. B **82**, 224106, (2010)

Ternary systems

- TM-TM-N:
  - Ti-V-N, Ti-Nb-N, Ti-Mo-N, Ti-W-N, Ti-Ta-N, V-W-N, V-Mo-N, V-Ta-N, D. G. Sangiovanni *et al.*, Acta Mater. **59**, 2121, (2011).
- TM-non-TM-N:
  - Ti-Al-N, P. H. Mayrhofer *et al.*, Appl. Phys. Lett. **83**, 2049, (2003).

Thank you!

Why the excitement now?

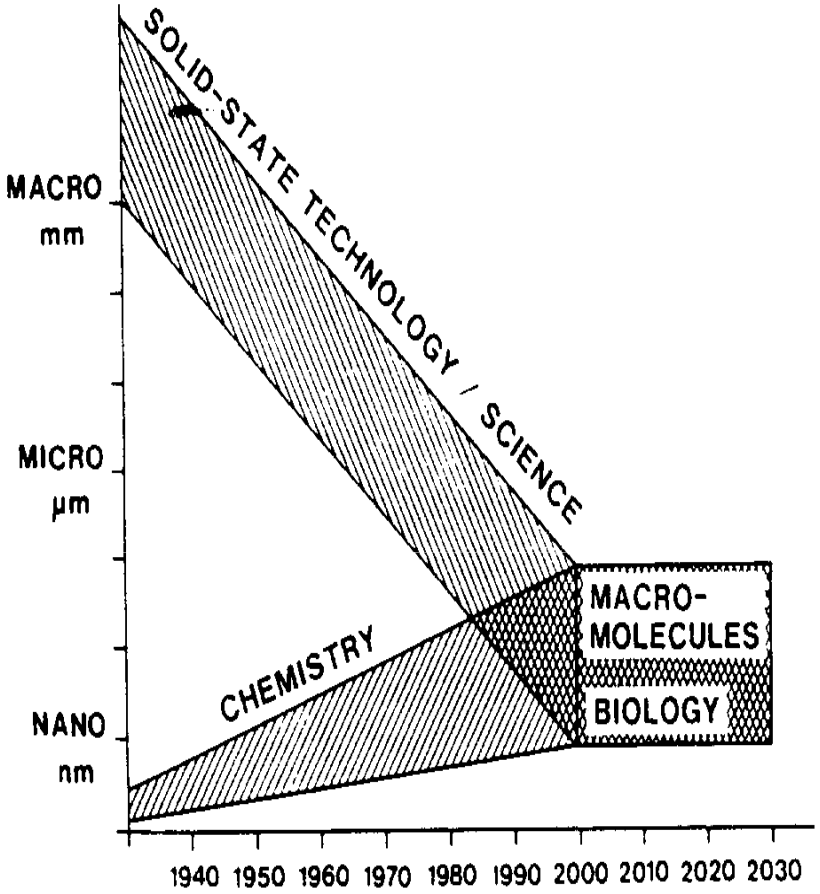

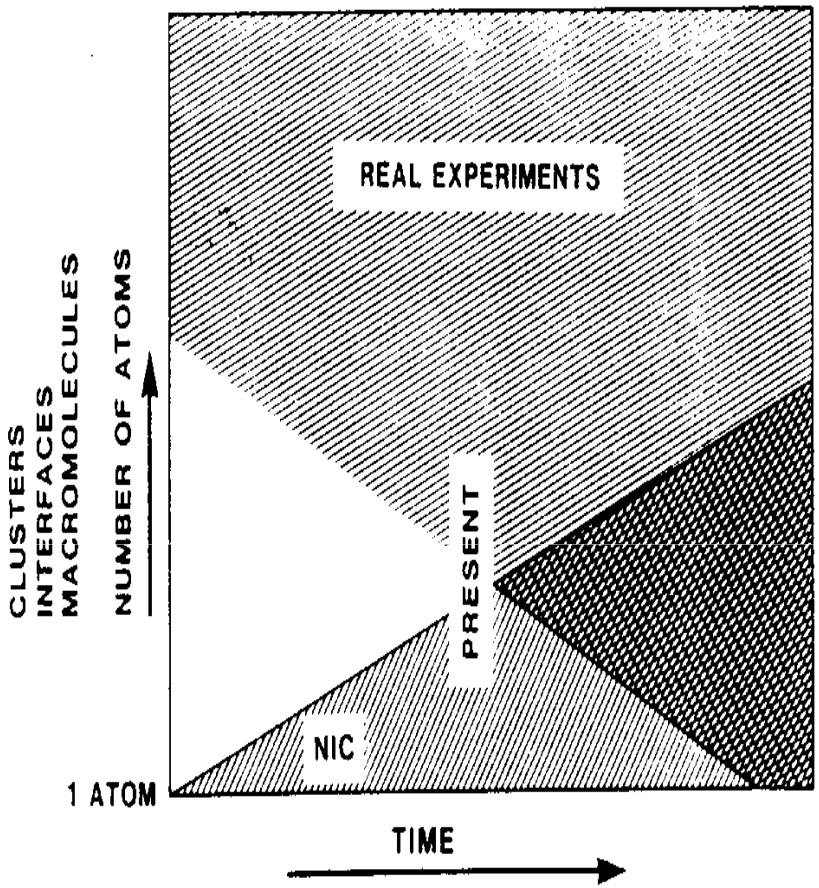

Convergence of device technology, physical instrumentation, chemical synthesis, biological assays, theory and computation.

Theoretical Techniques and Length Scales

- 10 – 100 nm and above: Continuum equations, FEM simulations, numerically solve PDEs, empirical relations.
- 1-10 nm: Monte Carlo Simulations, Molecular Dynamics, empirical potentials.
- < 1 nm *Ab initio* theory, fully quantum mechanical.
- Integrate appropriate and most important science from lower to higher scale.

Large length scale 100 nm

Length scale: 100 nm
Materials: Metals, semiconductors, metal nitrides (Ag, Pt, Si, Ge, TiN)
Phenomenon: Energetics, dynamics, fluctuations of steps, islands
Techniques: Analytical, Numerical solutions to PDEs, Monte Carlo

Example

Length scale: > 100 nm
Materials: surface of TiN(111)
Phenomenon: Dislocation driven surface dynamics
Techniques: Analytical model

Low energy electron micrographs of decay of two dimensional (2D) TiN islands on TiN(111)

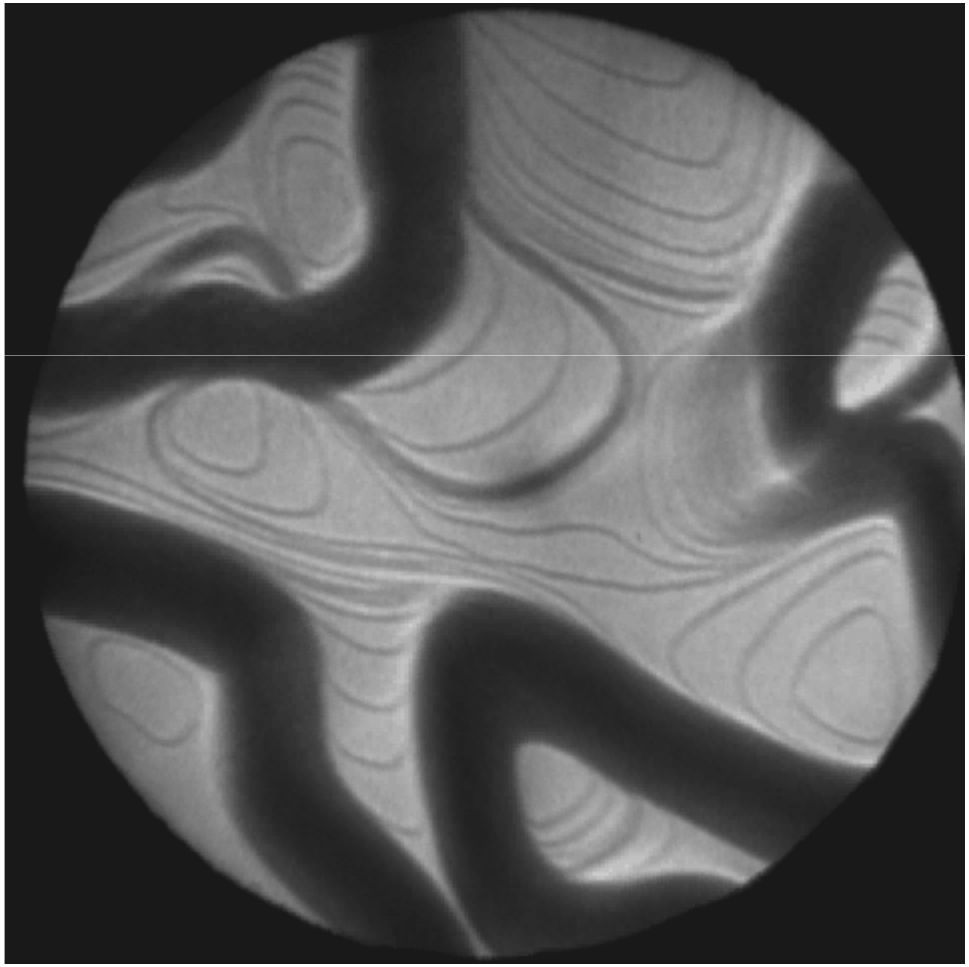

t_{real} = 12 min
t_{movie} = 17 sec

4×4 μm²

T_a = 1280 °C

Rate of area change
$dA/dt \sim \exp(-E_a/kT)$,

E_a = activation energy for atom detachment from step to terrace

Rate island area change dA/dt vs. temperature T

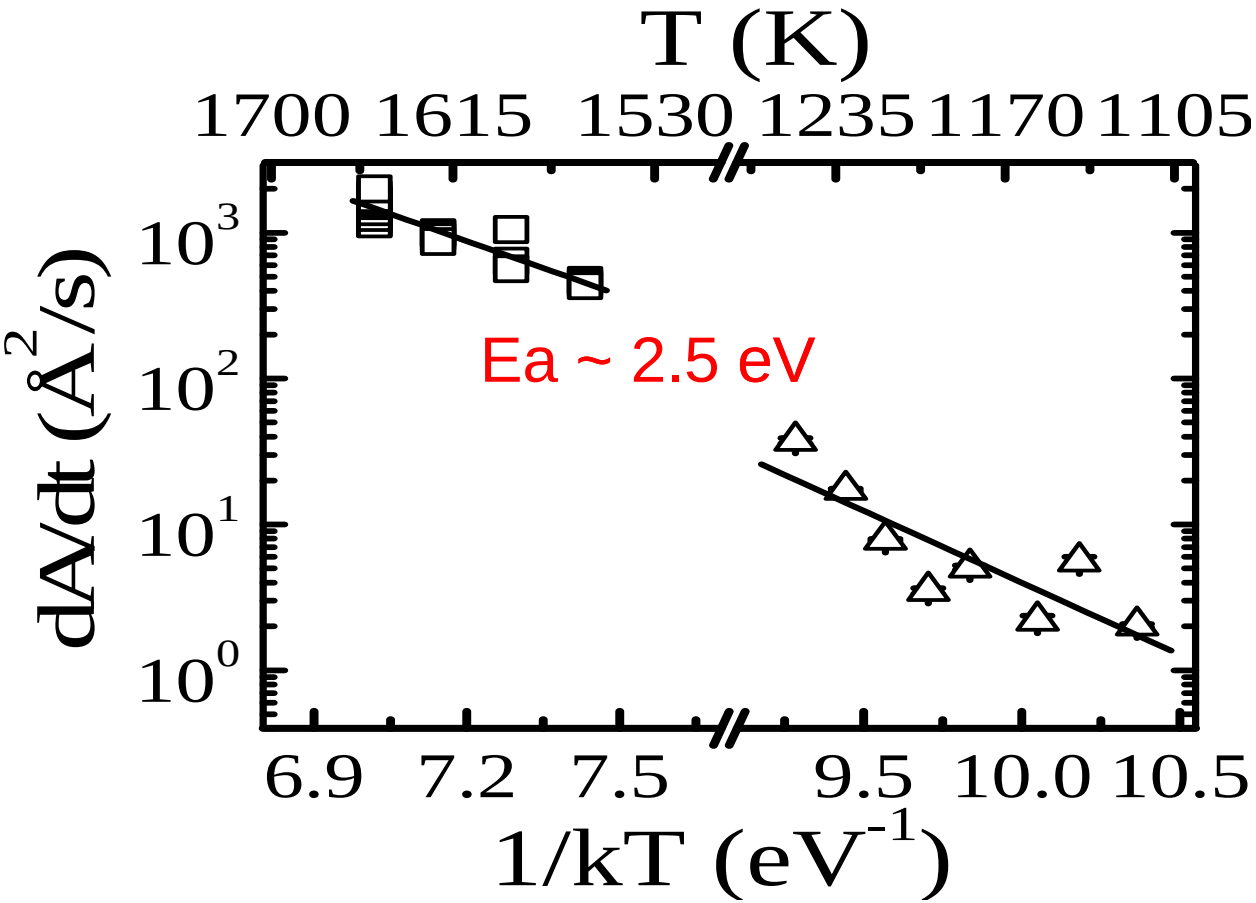

Measured E_a is in agreement with detachment limited step-curvature driven surface transport*

*S. Kodambaka, V. Petrova, S.V. Khare, D. Gall, A. Rockett, I. Petrov, and J.E. Greene, *Phys. Rev. Lett.* **89**, 176102 (2002).

Low energy electron micrographs of growth of spirals and loops of TiN on TiN(111)

$T/T_m \sim 0.5$

Spiral

T = 1415 °C

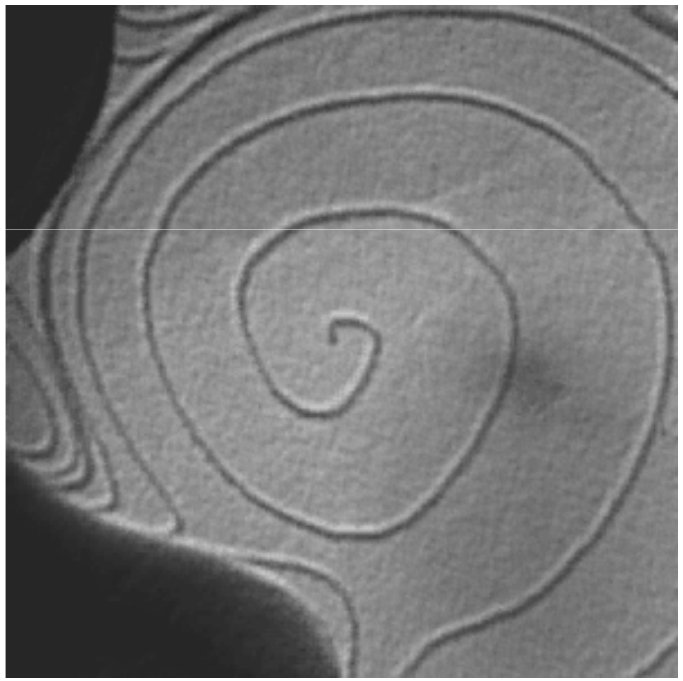

field of view: 2.5 μm

t_{real} = 90 s; t_{movie} = 9 s

2D Loop

T = 1380 °C

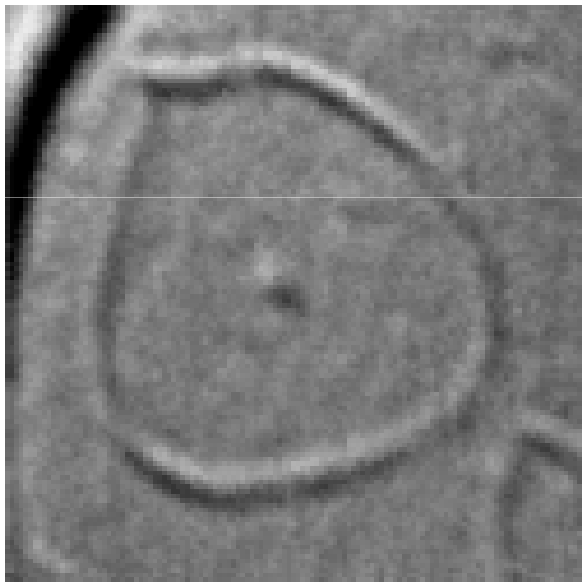

field of view: 1.0 μm

t_{real} = 200 s; t_{movie} = 21 s

2D Loop schematic

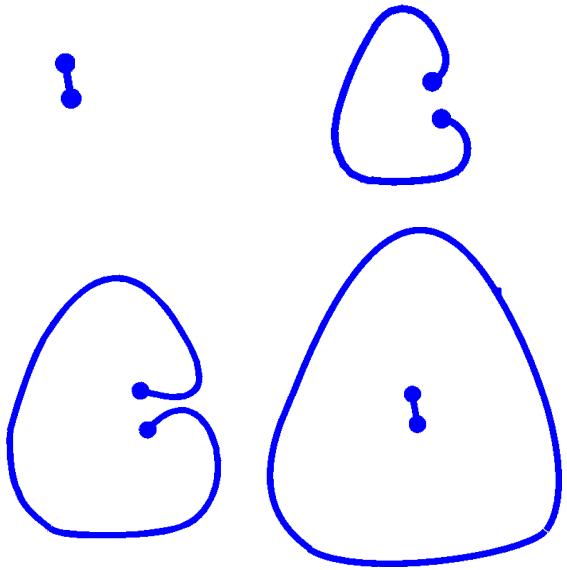

Not BCF growth structures

TiN/TiN(111)

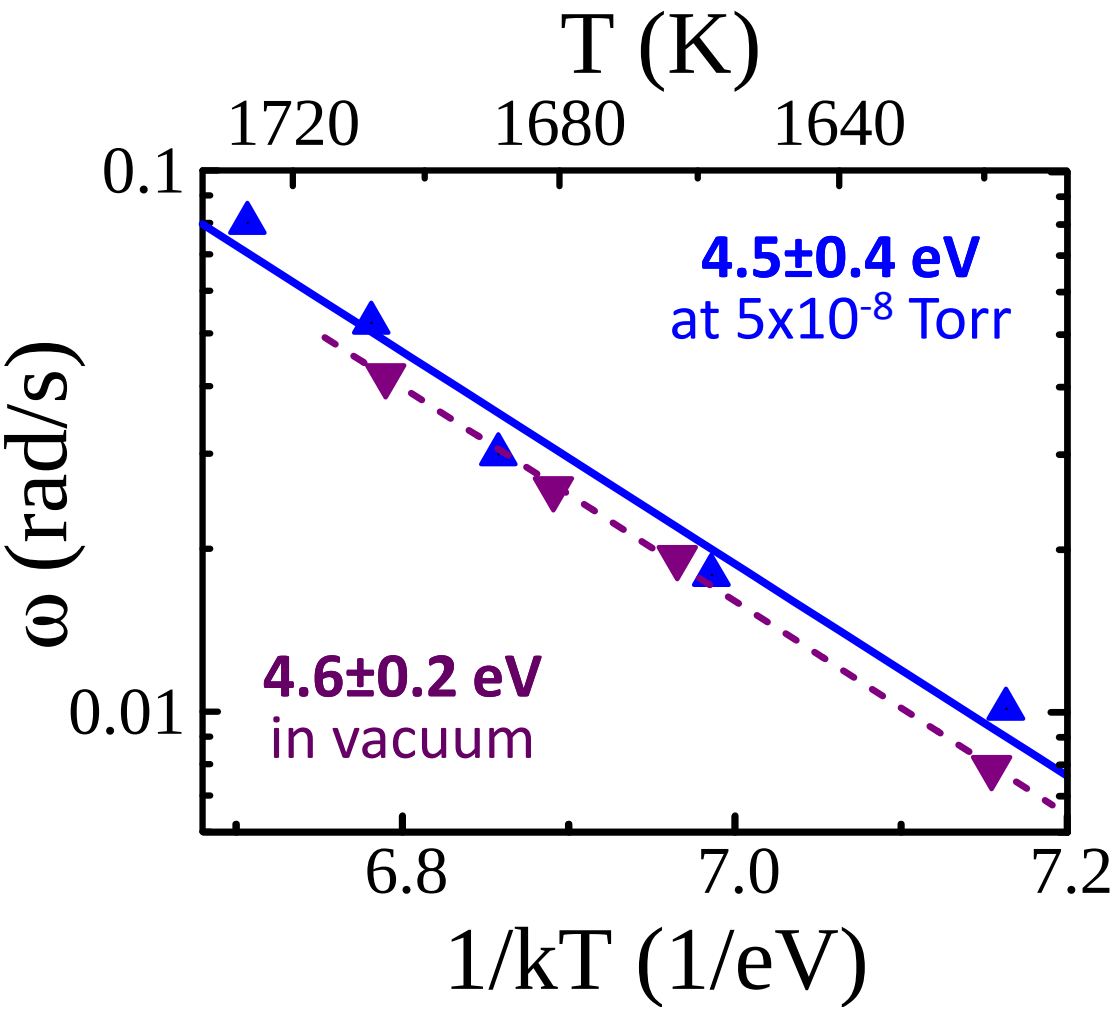

E_{spiral} is independent of N_2 pressure & sample history

Spirals Summary

- TiN(111) step dynamics and the effect of surface-terminated dislocations were studied using LEEM (1200-1500 ^{o}C).

- Spiral step growth kinetics: *qualitatively & quantitatively* different from 2D TiN(111) island decay.

- Mechanism: facile bulk point defect migration along the dislocations (E_d = 4.5±0.2 eV).

"Dislocation Driven Surface Dynamics on Solids," S. Kodambaka, S. V. Khare, W. Sweich, K. Ohmori, I. Petrov, and J. E. Greene, Nature, 429, 49 (2004);

"Nucleation and Growth Kinetics of Spiral Steps on TiN(111): an In-Situ Low-Energy Electron Microscopy Study," S. Kodambaka, J. Bareno, S. V. Khare, W. Swiech, I. Petrov, and J. E. Greene, J. Appl. Phys. 98, 34901 (2005).

Available at: http://www.physics.utoledo.edu/~khare/pubs/

MEDIA

ISOTROPIC

ε,μ are scalars

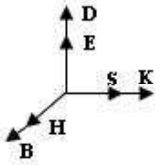

ANISOTROPIC

ε,μ are tensors

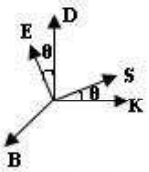

$$\varepsilon = \begin{bmatrix} \varepsilon_{xx} & \varepsilon_{xy} & \varepsilon_{xz} \\ \varepsilon_{yx} & \varepsilon_{yy} & \varepsilon_{yz} \\ \varepsilon_{zx} & \varepsilon_{zy} & \varepsilon_{zz} \end{bmatrix} \quad \mu = \begin{bmatrix} \mu_{xx} & \mu_{xy} & \mu_{xz} \\ \mu_{yx} & \mu_{yy} & \mu_{yz} \\ \mu_{zx} & \mu_{zy} & \mu_{zz} \end{bmatrix}$$

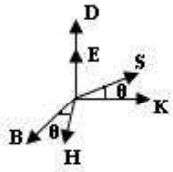

ε - anisotropic

μ - anisotropic

RECIPROCAL

$$\varepsilon = \begin{bmatrix} \varepsilon_1 & 0 & 0 \\ 0 & \varepsilon_2 & 0 \\ 0 & 0 & \varepsilon_3 \end{bmatrix} \quad \mu = \begin{bmatrix} \mu_1 & 0 & 0 \\ 0 & \mu_2 & 0 \\ 0 & 0 & \mu_3 \end{bmatrix}$$

NONRECIPROCAL

$$\varepsilon = \begin{bmatrix} \varepsilon_1 & j\varepsilon_4 & j\varepsilon_5 \\ -j\varepsilon_4 & \varepsilon_2 & j\varepsilon_6 \\ -j\varepsilon_5 & -j\varepsilon_6 & \varepsilon_3 \end{bmatrix} \quad \mu = \begin{bmatrix} \mu_1 & j\mu_4 & j\mu_5 \\ -j\mu_4 & \mu_2 & j\mu_6 \\ -j\mu_5 & -j\mu_6 & \mu_3 \end{bmatrix}$$

X-ray diffraction of PtN

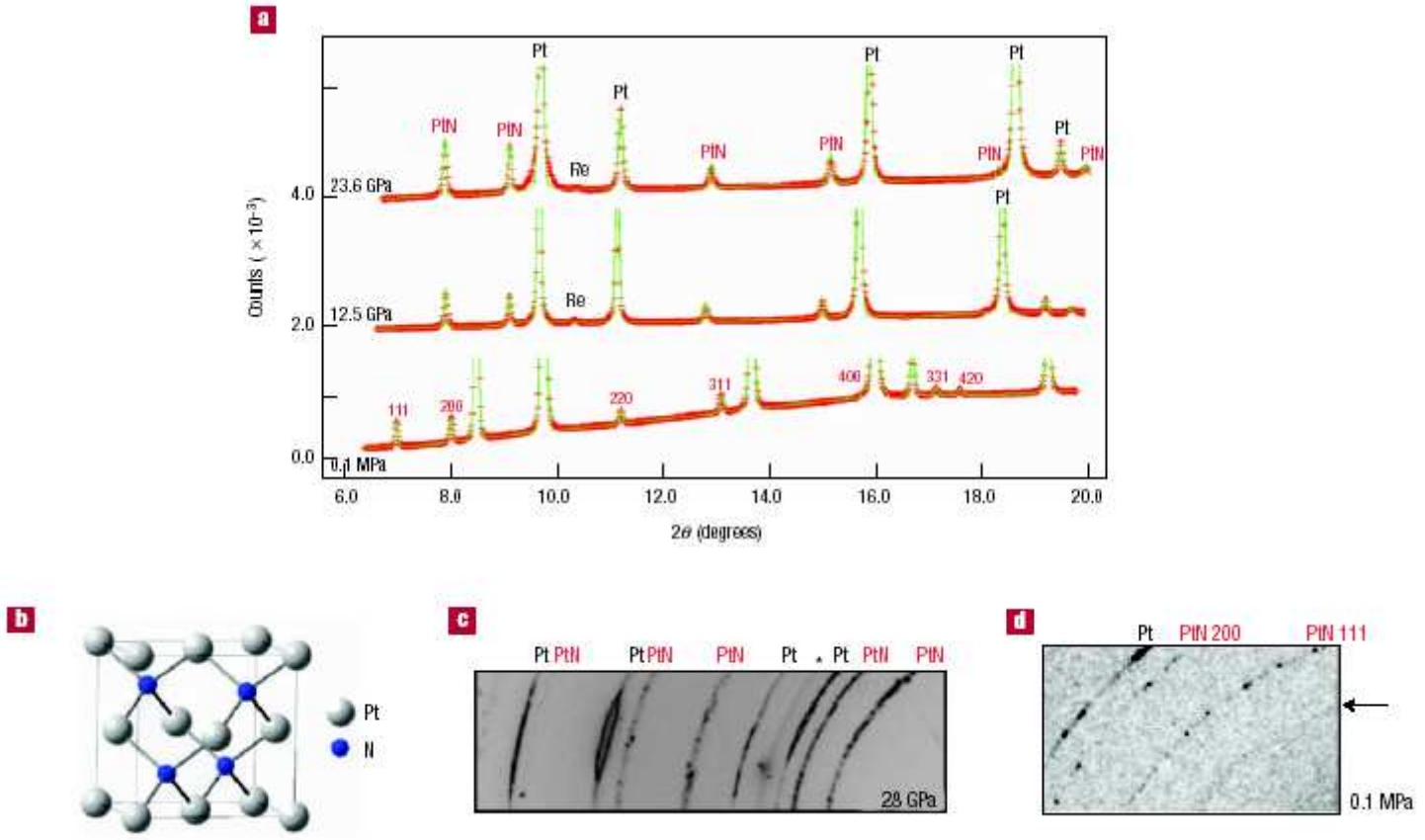

Figure 3 ***In situ*** **X-ray diffraction data. a**, X-ray spectra of PtN taken at different pressures.At ambient pressure the spectrum was taken with wavelength λ= 0.3311 Å and others with λ=0.3738 Å. Red crosses: data; green line: GSAS fit.**b**, Zinc-blende structure of PtN.**c**, Section of the CCD image at 28 GPa showing the powder-like texture; the asterisk indicates a rhenium diffraction ring. **d**, Detail of the inner section of the charged-coupled device image (shown in **c**) at ambient pressure with the arrow pointing at one of the two weak rings in addition to Pt and PtN signal.

Table III: Zinc-blende and rocksalt phases

MN	a (Å)	C_{11} (GPa)	C_{12} (GPa)	C_{44} (GPa)	B (GPa)	E (eV)
HfN (zb)	4.796	326.1	166.5	107.7	219.7	-23.25
(rs)	4.436	704.9	111.8	131.0	309.5	-24.11
TaN (zb)	4.659	314.9	258.8	13.0	274.2	-23.82
(rs)	4.326	826.9	155.9	73.4	379.6	-24.47
WN (zb)	4.584	unstable	unstable	unstable	308.3	unstable
(rs)	4.281	unstable	unstable	unstable	407.0	unstable
ReN (zb)	4.543	unstable	unstable	unstable	325.1	unstable
(rs)	4.276	unstable	unstable	unstable	403.4	unstable
OsN (zb)	4.527	unstable	unstable	unstable	327.2	unstable
(rs)	4.287	unstable	unstable	unstable	381.4	unstable
IrN (zb)	4.573	316.2	275.8	55.8	289.3	-17.99
(rs)	4.328	unstable	unstable	unstable	346.0	unstable
PtN (zb)	4.699	unstable	unstable	unstable	230.3	unstable
(rs)	4.407	355.0	248.0	36.0	284	-24.10
AuN (zb)	4.870	Unstable	Unstable	Unstable	161.1	Unstable
(rs)	4.5648	312.5	169.4	28.8	217.1	-10.31

All results with DFT-LDA